23

Late thrust propagation and sedimentary response in the thrust-belt–foredeep system of the Southern Apennines (Pliocene-Pleistocene)

Etta Patacca and Paolo Scandone

The progressive time–space migration of the Apennine thrust-belt–foredeep system and the consequent diachronism of the silicoclastic flysch deposits becoming younger toward the Po Plain–Adriatic foreland are basic concepts in the current geological literature, which have been assimilated over thirty years. This migration has been interpreted as a response to the flexure-hinge retreat of the subducting foreland lithosphere according to slip vectors largely exceeding the average plate-convergence rate in the Central Mediterranean region during Neogene and Quaternary times (Malinverno and Ryan, 1986; Patacca and Scandone, 1989; Patacca *et al.*, 1992a; Doglioni, 1991). Patacca and Scandone (1989) and Patacca *et al.* (1992c) have pointed out that cover detachment and nappe stacking did not proceed cylindrically along the Apennines, since adjacent segments of mountain chain, underlain by the same uninterrupted sole-thrust surface, may exhibit quite different structural architectures related to lateral changes of the thrust array. These different structural architectures may strongly influence the configuration of the foredeep sedimentary basin. Figure 23.1 shows two extreme cases. The first architecture is characterized by a stack of ramp anticlines mostly built up by piggy-back thrust propagation, while the second one is represented by the frontal part of a duplex system whose horses do not basically differ in shape and size from the previous imbricates. A pile of rootless nappes, which may display quite a complex internal geometry, overlies the duplex system. In Figure 23.1a a wide and deep foredeep basin is developed, the sedimentary record being potentially represented by a thick and wide clastic wedge mostly deposited by gravity-flow transport processes. The Miocene to lower Pliocene silicoclastic flysch deposits of the Northern Apenninic arc are typical products of this tectonic setting (Ricci Lucchi, 1986a,b; Patacca *et al.*, 1992a,c; Argnani and Ricci Lucchi, this vol., Ch. 19). In Figure 23.1b, in contrast, the front of the roof units has largely gone beyond the leading edge of the duplex system and the thrust toe (that is the portion of the tectonic wedge in front of the leading edge) occupies a considerable portion of the flexural depression. Consequently, the foredeep sedimentary basin ahead of the nappe front is narrower and shallower than the previous one and

G.B. Vai and I.P. Martini (eds.), Anatomy of an Orogen: the Apennines and Adjacent Mediterranean Basins, 401–440.

the space for potential sediments is drastically reduced. Very good subsurface examples of this second case, documented by seismic lines and well data, are represented by Pliocene and Pleistocene silicoclastic deposits which disconformably overlie the buried Apulia carbonates in the Bradano trough (Casnedi, 1988a,b). Possible small differences in the degree of curvature of the foreland plate between Figure 23.1a and Figure 23.1b have been neglected, owing to the small density contrast between the silicoclastic deposits filling the foredeep basin and the allochthonous sheets making up the thrust toe, as well as the subordinate contribution of the topographic load to the deflection of the Apulia lithosphere beneath the Apennines (Royden and Karner, 1984; Royden *et al.*, 1987; Royden, 1988; Moretti and Royden, 1988; Kruse and Royden, 1994).

The shape and size of the foredeep basins justify the most remarkable disparity between the two cases shown on Figure 23.1; nevertheless, other important differences in the sedimentary record appear when the entire tectonic evolution of the thrust system is considered. For example, if the frontal thrust is deactivated because of out-of-sequence thrust-propagation processes, the persisting flexural subsidence creates the same amount of accommodation space at the foot of the mountain chain in both cases in Figures 23.1a and 23.1b. However, in the first case only the outermost margin of the thrust belt is affected by a marine transgression, whilst in the second case a wide and flat area corresponding to the top of the thrust toe experiences widespread marine flooding. Once the system has been re-involved in the orogenic transport by forward (hinterland-to-foreland) thrust propagation, it is easy to mistake these thrust-sheet-top deposits, originally overlying a passive shelf, for thrust-sheet-top deposits filling a satellite basin which was forward limited by an active ridge (piggy-back basin; Ori and Friend, 1984).

This chapter deals with the relations between tectonics and sedimentation at the front of a mobile duplex system on top of the thrust toe and in the adjacent foredeep basin. The Campania–Lucania Apennines and the Bradano trough (the latter representing a deactivated and uplifted segment of the upper Pliocene to Middle Pleistocene foredeep basin) have been chosen as a case history for the following reasons:

(1) During the Middle Pleistocene, the flexural subsidence suddenly ceased in the Southern Apennines and the whole area underwent a

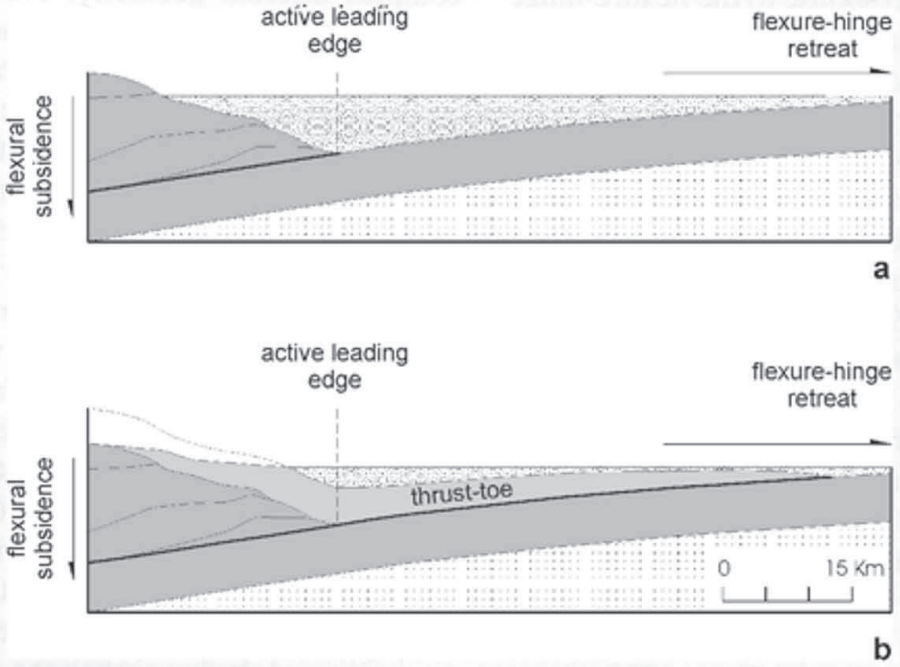

Figure 23.1 Schematic cross sections showing different configurations of foredeep basins produced by different styles of thrust propagation in the Apennines: A. Wide and deep depositional basin related to imbricate stack; B. Narrow and shallow basin in front of the thrust toe, related to duplex system overlain by rootless nappes.

considerable uplift accompanied by a gentle tilt toward the NE (Cinque *et al.*, 1993; Hippolyte *et al.*, 1994a). Because of considerable erosion, numerous natural sections have been exposed;

(2) A great deal of subsurface information is available because of the extensive hydrocarbon exploration in the Bradano trough and in the mountain chain (Crescenti, 1975; Balduzzi *et al.*, 1982a,b; Mostardini and Merlini, 1986, 1988; Casnedi, 1988a,b; Sella *et al.*, 1988, 1992; Casero *et al.*, 1991; D'Andrea *et al.*, 1993; Mattavelli *et al.*, 1993; Roure and Sassi, 1995; La Bella *et al.*, 1996);

(3) The high biostratigraphic resolution available in the Pliocene–Pleistocene deposits allows a detailed chronology of the deformation events;

(4) Although affected by compressional deformation, the Lower–Middle Pleistocene deposits of the Bradano trough unconformably overlying the outer margin of the Apennines have not been dismembered by the orogenic transport. The preservation of the original geometry of the thrust-belt–foredeep system makes the reconstruction of the synsedimentary tectonic activity more reliable.

The examples described in this chapter may offer a key to a better understanding of other segments of mountain chains where a similar tectonic evolution may have occurred, but information is not available from the subsurface or the original features have been greatly disrupted by structural deformation.

STRUCTURAL FRAMEWORK

The major upper Pliocene–Pleistocene stratigraphic and structural features of the Southern Apennines have been illustrated in Figures 23.2 and 23.3. Figure 23.2 gives some information on the subsurface tectonic structures; Figure 23.3 shows the major surface structural features and the distribution of the upper Pliocene to Quaternary deposits.

The base of the Pliocene to Pleistocene foredeep deposits in Figure 23.2, which deepens toward the mountain chain, matches the late flexural deflection of the Apulia foreland, although the original depth values of the isobaths have been slightly modified by the aforementioned Middle to Upper Pleistocene regional uplift (600–700 m at the outer margin of the Apennines, 300–350 m at the northeastern margin of the Bradano trough). NW–SE trending faults cutting across the rigid Apulia carbonates were formed during the late stages of flexure-hinge retreat, mostly during the Early Pleistocene. The buried front of the allochthonous sheets in Figure 23.2, roughly parallel to the NW–SE strike of the Apulia "homocline", is the tip line of the most external frontal ramp, active in earliest Pleistocene times (Santernian). It represents the termination of a long thrust flat responsible for the last forward (northeastward) displacement of the Apenninic nappes. This thrust surface joins the leading edge of a buried duplex system (Southern Apennine duplex system, Fig. 23.2) about 30 kilometres behind the nappe front, at depths exceeding 6000 m, in correspondence to the foot of a regionally developed thrust-fold cascade (Casero *et al.*, 1991; Roure *et al.*, 1991). This duplex system consists of a complex architecture of Apulia-carbonate horses overlain by rootless nappes, and forms the backbone of the Southern Apennine mountain chain.

Due to lateral variations of the thrust trajectories, the internal geometry of the Southern Apennines considerably changes along the strike of the mountain chain, even though the total shortening across adjacent sections displaying different thrust arrays may be approximately the same. Examples of different configurations caused by different trajectories of the active thrusts are given by the following.

(1) Bumpy-roof duplex structures, in which a stack of overlapping ramp anticlines developed in the Apulia carbonates has passively corrugated the roof thrust. A good example of this configuration is the Monte Forcuso structure (Fig. 23.2) where the top of the carbonates reaches shallow depth, lower than 1500 m below sea level (bsl). The complex internal geometry of this duplex structure has been accommodated above the roof thrust by a large antiform in the Apenninic nappes.

(2) Thick (more than 5000 m) antiformal stacks developed in the Apenninic nappes because of breaching of the duplex system and duplexing of the roof units; that is, of the allochthonous sheets overlying the roof thrust of the buried carbonate

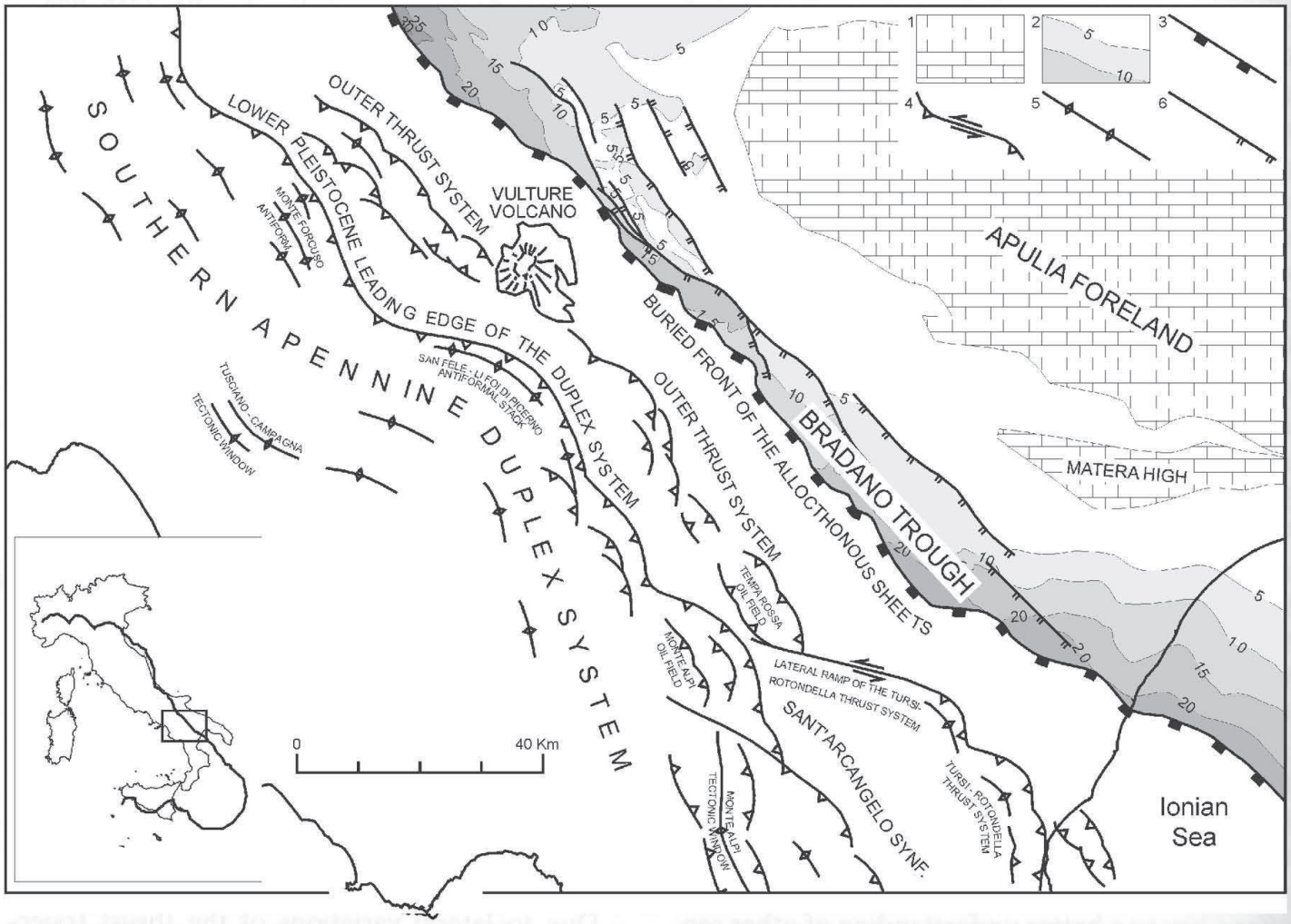

Figure 23.2 Map showing major subsurface tectonic features in the Southern Apennines (after Sella *et al.*, 1990; Casero *et al.*, 1992) (1, autochthonous Mesozoic–Tertiary carbonates of the Apulia foreland; 2, base of the Pliocene and Pleistocene deposits in the Bradano trough (isobaths in hundreds of metres); 3, front of the Apenninic nappes; 4, thrust fault (frontal/oblique and lateral ramps); 5, ramp anticline, antiformal stack and emergence of the deformed Apulia carbonates in correspondence to major culmination of the Apennine duplex system (Monte Alpi tectonic window); 6, strikeslip/ transpressional fault and (barbed line) normal fault).

duplex system. A good example is represented by the San Fele–Li Foi di Picerno antiformal stack developed within the Lagonegro nappes (Fig. 23.2).

Just behind the nappe front, tight imbricate structures are developed in the thrust toe from the northernmost part of the study area to the northern margin of a wide structural depression (Sant'Arcangelo synform) filled with Pliocene–Pleistocene deposits, known in the geological literature as the Sant'Arcangelo basin (Vezzani, 1967). These imbricates, limited by steep ramps with traces that are shown in Figure 23.3, are the result of repeated breaching processes which took place during the Pliocene and Pleistocene and produced a considerable telescopic shortening of the allochthonous sheets. The youngest and most continuous breach (Stigliano ramp) developed around the Early-Middle Pleistocene boundary. The surface trace of this ramp is almost continuously exposed for more than 100 km, from the Vulture volcano region to the Sauro valley (Fig. 23.3). At the Sauro River, the Stigliano ramp and the other frontal imbricates abruptly terminate against a sinistral strike-slip fault (Scorciabuoi fault) that marks the northern termination of the Sant'Arcangelo synform. This large structural depression has been interpreted either as a satellite basin forward (eastward) limited by active thrust structures (Camarlinghi 1992; Hippolyte *et al.*, 1991, 1994b; Pieri *et al.*, 1994) or as a pull-apart basin generated by sinistral strike-slip faults (Turco *et al.*, 1990). Cippitelli (1997) describes the

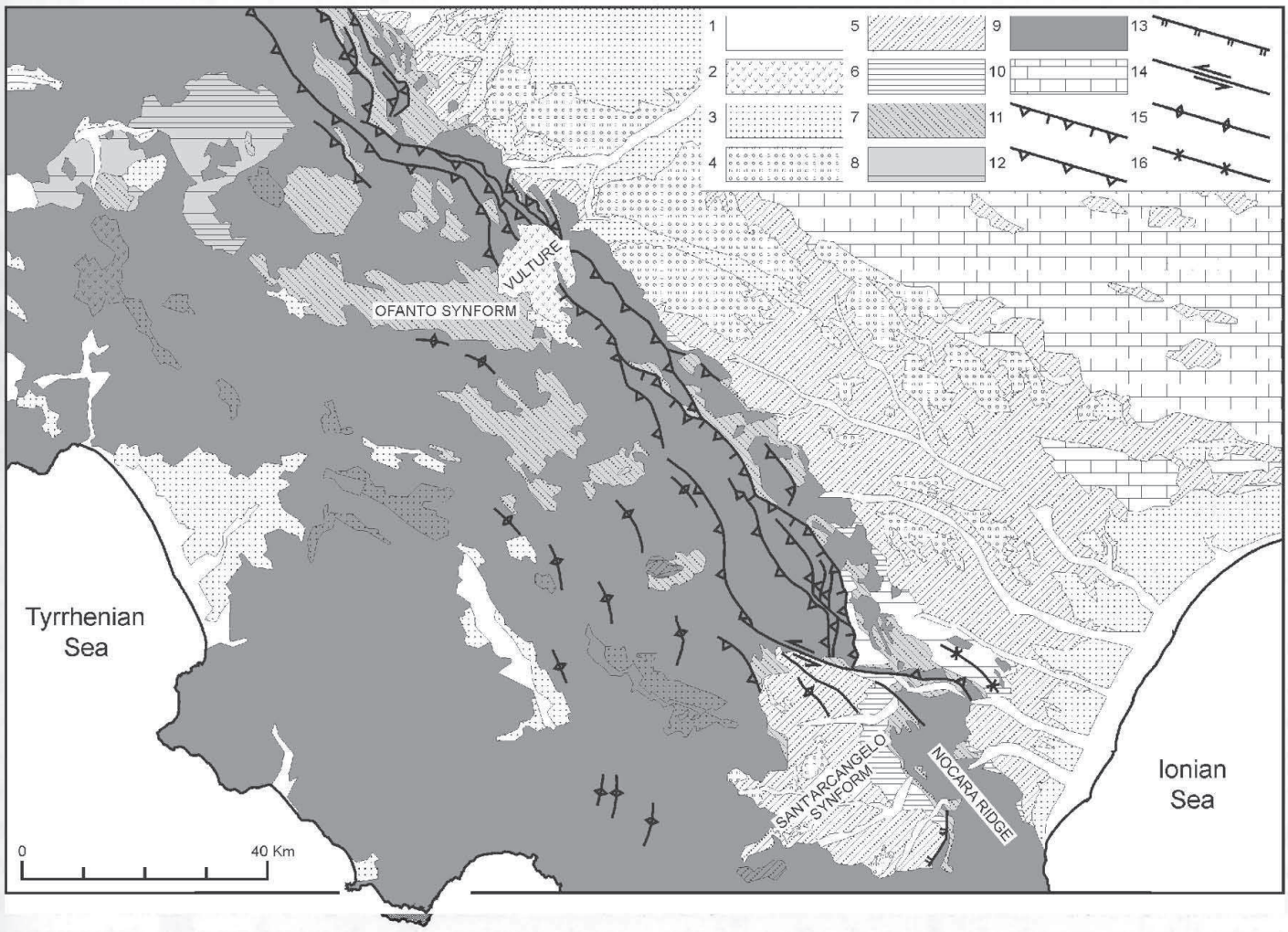

Figure 23.3 Map showing the major surface tectonic features and the distribution of the upper Pliocene–Pleistocene deposits in the Southern Apennines (1, alluvial and subordinate shore deposits (Holocene); 2, volcanites and volcanoclastic deposits (Middle–Late Pleistocene); 3, terraced continental and shallow-marine sedimentary units formed during a period of generalized deflexural uplift and severe block faulting in the mountain chain (Middle–Late Pleistocene); 4, continental to shallow-marine sedimentary units formed during an early stage of deflexural uplift (Serra Corneta and Irsina conglomerates, Middle Pleistocene around 0.65 Ma) and during a short period of tectonic quiescence (Monte Marano Sandstone, Middle Pleistocene, 0.66–0.65 Ma); 5, continental to marine sedimentary units formed on top of the allochthonous sheets, in the foredeep basin and on the foreland ramp after the last displacement of the Apenninic nappes towards the Apulia foreland, during a time interval characterized by thrust faulting behind the nappe front (Early–Middle Pleistocene, 1.50–0.66 Ma); 6, marine sedimentary units formed on top of the Apenninic nappes during their last displacement towards the Apulia foreland (Early Pleistocene, 1.83–1.50 Ma); 7, continental to marine sedimentary units formed on top of the allochthonous sheets during a time interval characterized by thrust faulting behind the nappe front (late Pliocene, 3.30–1.83 Ma) preceded and followed by major events of nappe displacement towards the Apulia foreland; 8, marine sedimentary units formed on top of the Apenninic nappes during their displacement towards the Apulia foreland in early–late Pliocene times (early–late Pliocene, 3.70–3.30 Ma); 9, Apenninic nappes and thrust-sheet-top deposits older than 3.70 Ma; 10, Mesozoic carbonates of the Apulia foreland; 11 and 12, Pliocene and Lower–Middle Pleistocene thrusts (11, Stigliano ramp); 13, normal fault; 14, strike-slip fault (arrows mark the Scorciabuoi left-lateral fault); 15, anticline axis; 16, syncline axis).

Sant'Arcangelo synform as a pull-apart basin eastward limited by a structural high created by a deep-seated mafic intrusion. The synform is separated from the Bradano trough by a NW–SE trending structural high (Nocara ridge in Fig. 23.3) grown on top of a system of ramp anticlines and associated back-thrust structures in the Apulia carbonates (Tursi–Rotondella thrust system, Fig. 23.2). In this thrust system, formed near the Early–Middle Pleistocene boundary, the top of the buried Apulia carbonates lies at very shallow depths (less than 1500 m bsl in Montegiordano 1 AGIP, between 1500 and 2000 m in the Rotondella 1 2 and 4 wells, and at a depth slightly exceeding

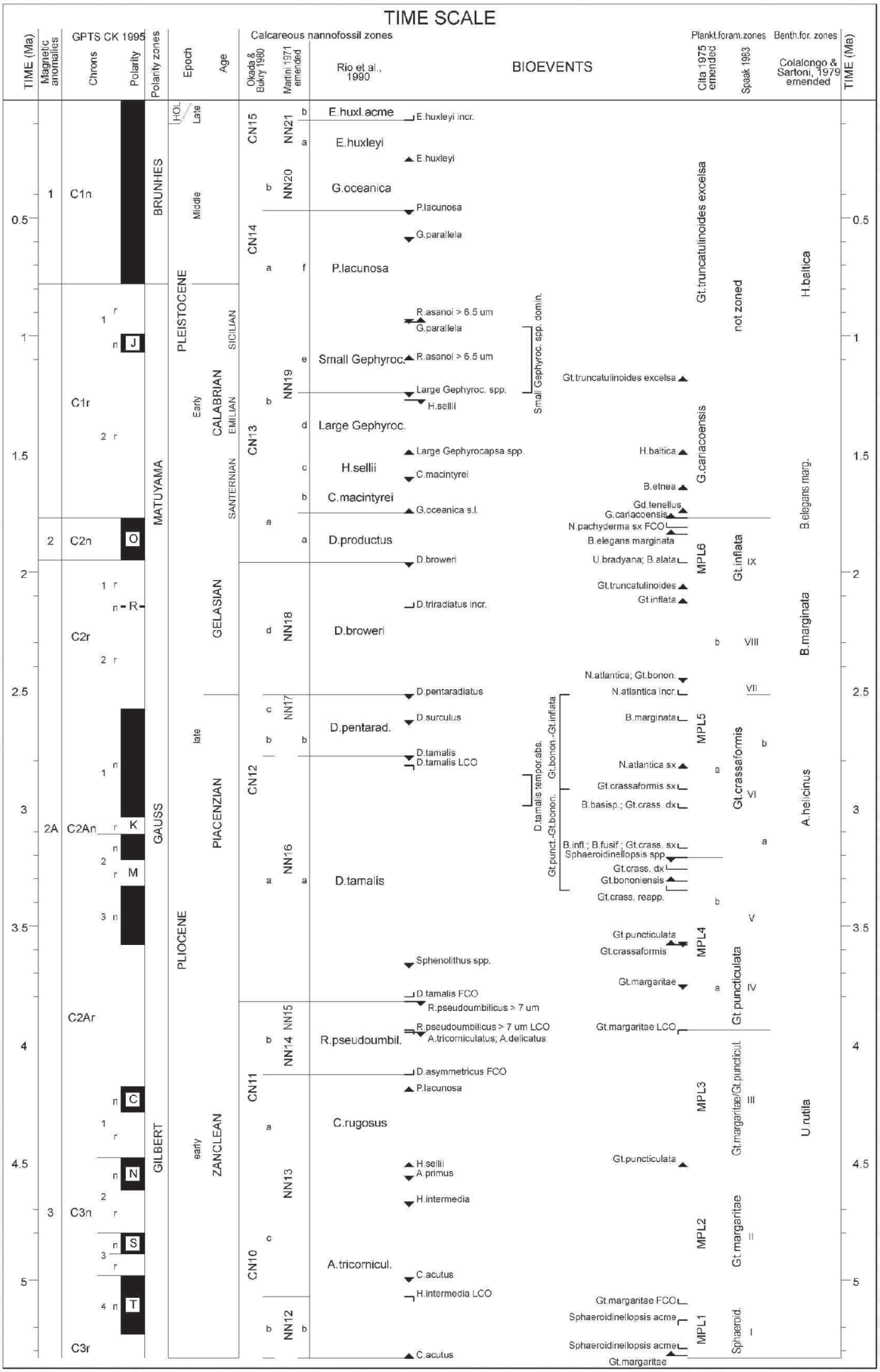
TIME SCALE
TIME (Ma)
Magnetic anomalies
GPTS CK 1995
Chrons
Polarity
Polarity zones
Epoch
Age
Calcareous nannofossil zones
Okada & Bukry 1980
Martini 1971 emended
Rio et al., 1990
BIOEVENTS
Plankt.foram.zones
Cita 1975 emended
Spaak 1983
Benth.for. zones
Colalongo & Sartoni, 1979 emended
BRUNHES
MATUYAMA
GAUSS
GILBERT
PLEISTOCENE
PLIOCENE
HOL.
Late
Middle
Early
late
early
SICILIAN
CALABRIAN
EMILIAN
SANTERNIAN
GELASIAN
PIACENZIAN
ZANCLEAN
CN15
CN14
CN13
CN12
CN11
CN10
NN21
NN20
NN19
NN18
NN17
NN16
NN15
NN14
NN13
NN12
E.huxl.acme
E.huxleyi incr.
E.huxleyi
G.oceanica
P.lacunosa
G.parallela
R.asanoi > 6.5 um
Small Gephyroc.
Large Gephyroc. spp.
H.sellii
Large Gephyroc.
Large Gephyrocapsa spp.
H.sellii
C.macintyrei
C.macintyrei
G.oceanica s.l.
D.productus
D.broweri
D.triradiatus incr.
D.broweri
D.pentaradiatus
D.surculus
D.pentarad.
D.tamalis
D.tamalis LCO
D.tamalis
Sphenolithus spp.
D.tamalis FCO
R.pseudoumbilicus > 7 um
R.pseudoumbilicus > 7 um LCO
R.pseudoumbil.
A.tricorniculatus; A.delicatus
D.asymmetricus FCO
P.lacunosa
C.rugosus
H.sellii
A.primus
H.intermedia
A.tricornicul.
C.acutus
H.intermedia LCO
C.acutus
Small Gephyroc. spp. domin.
D.tamalis tempor.abs.
Gt.punct.-Gt.bonon.
Gt.bonon.-Gt.inflata
Gt.truncatulinoides excelsa
H.baltica
B.etnea
Gd.tenellus
G.cariacoensis
N.pachyderma sx FCO
B.elegans marginata
U.bradyana; B.alata
Gt.truncatulinoides
Gt.inflata
N.atlantica; Gt.bonon.
N.atlantica incr.
B.marginata
N.atlantica sx
Gt.crassaformis sx
B.basisp.; Gt.crass. dx
B.infl.; B.fusif.; Gt.crass. sx
Sphaeroidinellopsis spp.
Gt.crass. dx
Gt.bononiensis
Gt.crass. reapp.
Gt.puncticulata
Gt.crassaformis
Gt.margaritae
Gt.margaritae LCO
Gt.puncticulata
Gt.margaritae FCO
Sphaeroidinellopsis acme
Sphaeroidinellopsis acme
Gt.margaritae
Gt.truncatulinoides excelsa
G.cariacoensis
MPL6
MPL5
MPL4
MPL3
MPL2
MPL1
not zoned
Gt.inflata
Gt.crassaformis
Gt.puncticulata
Gt.margaritae/Gt.puncticul.
Gt.margaritae
Sphaeroid.
IX
VIII
VII
VI
V
IV
III
II
I
H.baltica
B.elegans marg.
B.marginata
A.helicinus
U.rutila
C1n
C1r
C2n
C2r
C2An
C2Ar
C3n
C3r
J
O
R
K
M
C
N
S
T
1
2
2A
3
0.5
1
1.5
2
2.5
3
3.5
4
4.5
5

Table 23.1 Biochronology of late Neogene to Quaternary calcareous nannofossils.

Datum event	Reference	Age (Ma)
Emiliania huxleyi increase	Shipboard Scientific Party, 1995. Explanatory notes	0.085
Emiliania huxleyi FO	Shackleton *et al.*, 1995	0.26
Pseudoemiliania lacunosa LO	Castradori, 1993	0.468
Gephyrocapsa parallela LO	Castradori, 1993	0.584
Reticulofenestra asanoi >6.5 μm LO	Shipboard Scientific Party, 1996. Explanatory notes	0.93
Gephyrocapsa parallela FO	Castradori, 1993	0.94
Small *Gephyrocapsa* spp. end dominance	Berggren *et al.*, 1995	0.96
Reticulofenestra asanoi >6.5 μm FO	Shipboard Scientific Party, 1996. Explanatory notes	1.10
Small *Gephyrocapsa* spp. beginning dominance	Berggren *et al.*, 1995	1.24
Large *Gephyrocapsa* spp. LO	Shipboard Scientific Party, 1995. Explanatory notes	1.24
Helicosphaera sellii LO	Shipboard Scientific Party, 1996. Explanatory notes	1.27
Large *Gephyrocapsa* spp. FO	Sprovieri, 1993	1.50
Calcidiscus macintyrei LO	Shipboard Scientific Party, 1995. Explanatory notes	1.60
Gephyrocapsa oceanica sl. FO	Sprovieri, 1993	1.75
Discoaster broweri LO	Shackleton *et al.*, 1995	1.96
Discoaster triradiatus increase	Shipboard Scientific Party, 1996. Explanatory notes	2.15
Discoaster pentaradiatus LO	Shackleton *et al.*, 1995	2.52
Discoaster surculus LO	Shackleton *et al.*, 1995	2.63
Discoaster tamalis LO	Shackleton *et al.*, 1995	2.78
Discoaster tamalis LCO	Sprovieri, 1993	2.82
Discoaster tamalis temporary absence end	Sprovieri, 1993	2.86
Discoaster tamalis temporary absence begin	Sprovieri, 1993	2.99
Sphenolithus spp. LO	Shackleton *et al.*, 1995	3.66
Discoaster tamalis LCO	Shipboard Scientific Party, 1996. Explanatory notes	3.80
Reticulofenestra pseudoumbilicus >7 μm LO	Shackleton *et al.*, 1995	3.82
Reticulofenestra pseudoumbilicus >7 μm LCO	Shipboard Scientific Party, 1996. Explanatory notes	3.94
Amaurolithus tricorniculatus LO	Shipboard Scientific Party, 1996. Explanatory notes	3.95
Amaurolithus delicatus LO	Shipboard Scientific Party, 1996. Explanatory notes	3.95
Discoaster asymmetricus FCO	Shackleton *et al.*, 1995	4.13
Pseudoemiliana lacunosa FO	Shipboard Scientific Party, 1996. Explanatory notes	4.20
Helicosphaera sellii FO	Shipboard Scientific Party, 1996. Explanatory notes	4.52
Amaurolithus primus LO	Shackleton *et al.*, 1995	4.56
Helicosphaera intermedia LO	Shipboard Scientific Party, 1996. Explanatory notes	4.67
Ceratolithus acutus LO	Shackleton *et al.*, 1995	4.99
Helicosphaera intermedia LCO	Shipboard Scientific Party, 1996. Explanatory notes	5.07
Ceratolithus acutus FO	Shackleton *et al.*, 1995	5.33

line drawing in Figure 23.12. The Pliocene–Pleistocene deposits have been grouped into a lower–upper Pliocene (P_{1-2}) and a Lower– Middle Pleistocene (Q_{1-2}) tectonically-controlled depositional sequences. Both sequences have been divided into different systems tracts according to depositional architectures determined by the synsedimentary thrust propagation.

Northern transect

The northern transect (Figs 23.5, 23.7, 23.9, 23.10) extends from the outer flank of the San Fele antiformal stack (Fig. 23.2) to the Apulia foreland. The transect cuts across the Ofanto synform, the imbricate structures of the thrust toe, the buried front of the allochthonous sheets and the adjacent foredeep basin.

The Ofanto synform has been described by Hippolyte *et al.* (1994b) and Roure *et al.* (1991) as a polyphase satellite basin formed on top of the Apenninic nappes in early–middle Pliocene times (NN15–NN16 nannofossil zones). According to these authors, the basin evolution was initially characterized by a progressive backward (southward) migration of the depocentre. This was determined by the geometry of the active thrust surface, which consists of a W–E trending deep ramp at the rear of the basin and a shallow ramp in front of it, the basin itself overlying a short flat

Table 23.2 Biochronology of late Neogene to Quaternary planktic foraminifera.

Datum event	Reference	Age (Ma)
Globorotalia truncatulinoides excelsa FO	Sprovieri, 1993	1.19
Globigerinoides tenellus FO	Pasini and Colalongo, 1982, 1994	1.75
Globigerina cariacoensis FO	Berggren *et al.*, 1995	1.77
Neogloboquadrina pachyderma sinistral FCO	Sprovieri, 1993	1.81
Globorotalia truncatulinoides FO	Sprovieri, 1993	2.07
Globorotalia inflata FO	Sprovieri, 1993	2.13
Globorotalia bononiensis LO	Sprovieri, 1993	2.45
Neogloboquadrina atlantica sinistral FO	Sprovieri, 1993	2.45
Neogloboquadrina atlanctica increase	Rio *et al.*, 1990	2.52
Globorotalia bononiensis–Globorotalia inflata intermediate morphotypes (disappearance)	Spaak, 1983	2.52
Neogloboquadrina atlantica FO	Sprovieri, 1993	2.83
Globorotalia bononiensis–Globorotalia inflata intermediate morphotypes (appearance)	Spaak, 1983	2.92
Globorotalia puncticulata–Globorotalia bononiensis intermediate morphotypes (disappearance)	Spaak, 1983	2.92
Globorotalia crassafomis dextral to sinistral coiling change	Berggren *et al.*, 1995	2.92
Globorotalia crassafomis sinistral to dextral coiling change	Berggren *et al.*, 1995	3.00
Globorotalia crassafomis dextral to sinistral coiling change	Berggren *et al.*, 1995	3.17
Sphaeroidinellopsis spp. LO	Berggren *et al.*, 1995	3.21
Globorotalia crassafomis sinistral to dextral coiling change	Berggren *et al.*, 1995	3.26
Globorotalia bononiensis FO	Sprovieri, 1993	3.31
Globorotalia crassaformis reappearance	Berggren *et al.*, 1995	3.35
Globorotalia puncticulata–Globorotalia bononiensis intermediate morphotypes (appearance)	Spaak, 1983	3.35
Globorotalia puncticulata LO	Sprovieri, 1993	3.57
Globorotalia crassaformis FO	Berggren *et al.*, 1995	3.58
Globorotalia margaritae LO	Sprovieri, 1993	3.75
Globorotalia margaritae LCO	Sprovieri, 1993	3.94
Globorotalia puncticulata FO	Sprovieri, 1993	4.52
Globorotalia margaritae FCO	Sprovieri, 1993	5.10
Sphaeroidinellopsis spp. acme end	Di Stefano *et al.*, 1996	5.17
Sphaeroidinellopsis spp. acme beginning	Di Stefano *et al.*, 1996	5.29

Table 23.3 Biochronology of selected late Neogene to Quaternary benthic foraminifera.

Datum event	Reference	Age (Ma)
Hyalinea baltica FO	Pasini and Colalongo, 1982, 1994	1.50
Bulimina etnea FO	Pasini and Colalongo, 1982, 1994	1.65
Bulimina elegans marginata FO	Pasini and Colalongo, 1982, 1994	1.84
Uvigerina bradyana FCO	Original data	1.96*
Brizalina alata FCO	Original data	1.96*
Bulimina marginata FCO	Original data	2.63*
Bulimina basispinosa FCO	Original data	3.00*
Bulimina inflata FCO	Original data	3.17*
Bulimina fusiformis FCO	Original data	3.17*

that linked the two ramps. Later (late Pliocene, NN18 nannofossil zone), the basin depocentre underwent a northeastward migration because of a considerable tilt of the southeastern margin of the synform caused by the growth of a nappe anticline in correspondence to the San Fele structure.

Our interpretation of the Ofanto synform does not fully conform to this reconstruction because

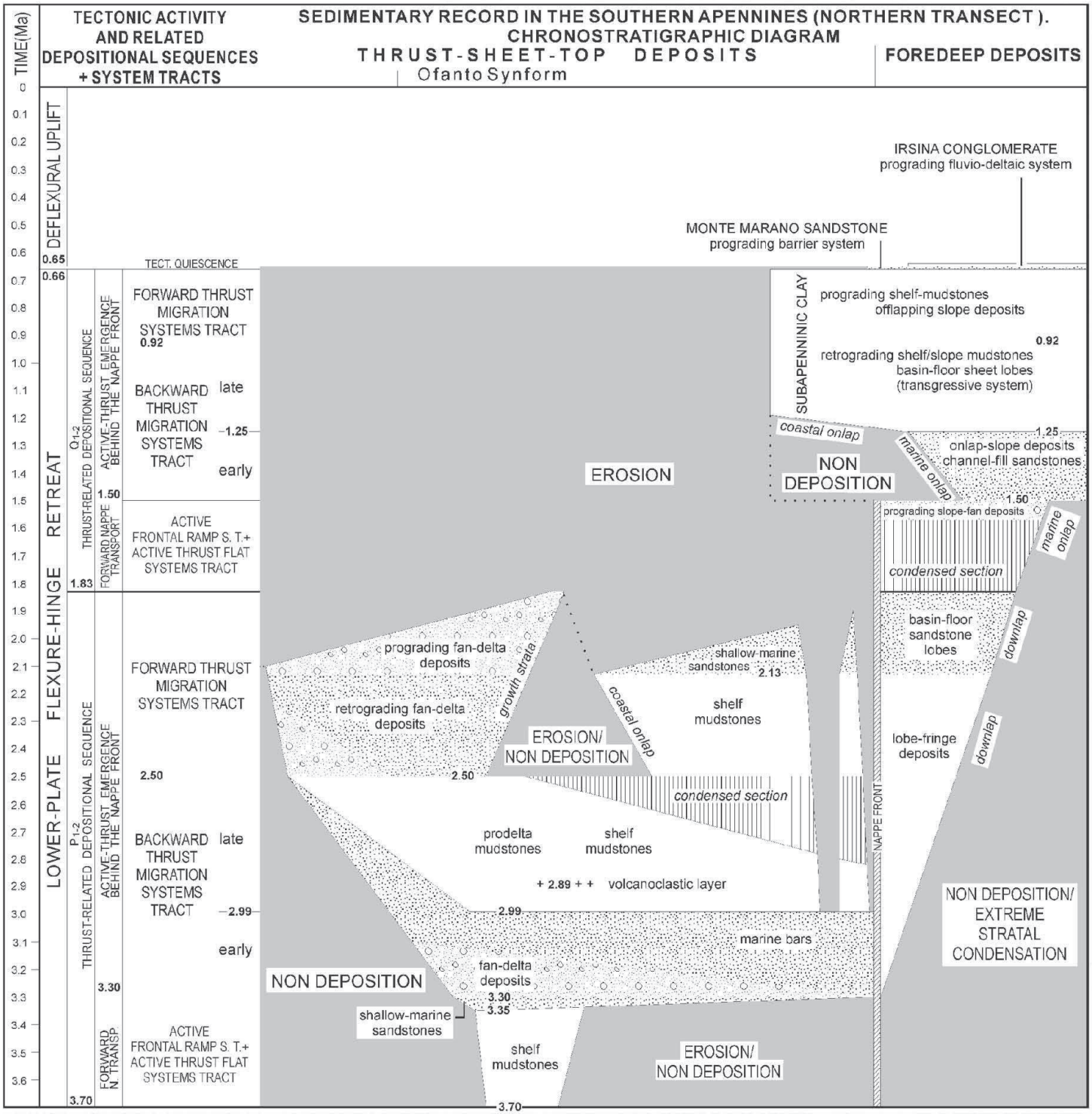

Figure 23.5 Chronostratigraphic diagram summarizing the lower–upper Pliocene to Middle Pleistocene sedimentary record in the Southern Apennines along a transect across the Ofanto synform (Fig. 23.3), the buried front of the allochthonous sheets and the adjacent foredeep basin in the Vulture volcano region.

the facies and the internal geometry of the analysed thrust-sheet-top deposits indicate a more complex kinematic evolution. We have distinguished several groups of Pliocene sedimentary units with depositional attributes that appear to have been controlled by different tectonic settings.

The first group of Pliocene deposits, widely exposed in the Ariano and Benevento areas a few tens of kilometres NW of the trace of the northern transect (units 7e and 7f, Fig. 23.7), has been recognized in the Ofanto synform only on seismic profiles (Fig. 23.10). In the Benevento and Ariano areas, the stratigraphic sequence is represented by lower/upper Pliocene open-shelf foraminiferal mudstones and shallow-marine sandstones (3.70–3.30 Ma interval, Figs 23.5). The mudstone–

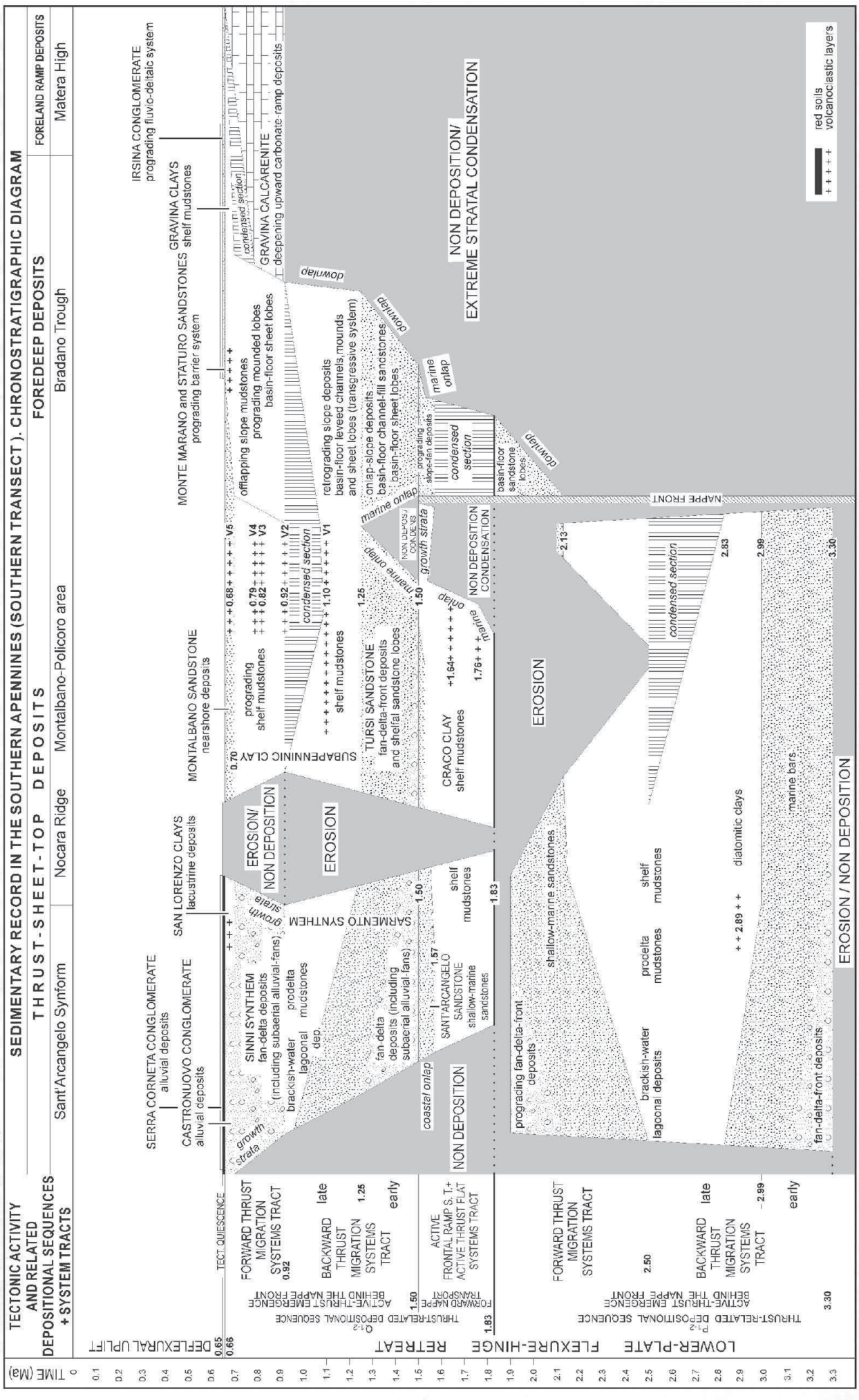

Figure 23.6 Chronostratigraphic diagram summarizing the upper Pliocene to Middle Pleistocene sedimentary record in the Southern Apennines along a transect across the Sant'Arcangelo synform (Fig. 23.3), the buried front of the allochthonous sheets and the adjacent foredeep basin close to the Ionian Sea coast.

sandstone couplet forms an overall shallowing-upward sequence that drapes the allochthonous sheets without significant lateral variations in facies and thickness. The foraminiferal assemblage (*Sphaeroidinellopsis* spp. in co-occurrence with *Globorotalia puncticulata*) and the nannofossil association (*Sphenolithus* spp. together with *Discoaster tamalis*) present in the lower part of the mudstones justify the attribution of these deposits to the lower portion of the NN16a nannofossil zone above the disappearance of *Globorotalia margaritae*. The upper portion of the mudstones is temporally constrained by a nannofossil assemblage indicative of the NN16a zone above the disappearance of *Sphenolithus* spp. and by a foraminiferal association pointing to the Spaak's V zone (*Sphaeroidinellopsis* spp. associated with *Globorotalia aemiliana* and absence of *Gt. puncticulata*). The basal layers of the overlying shelf sandstones yield *Uvigerina rutila* in association with *Globorotalia puncticulata–Globorotalia bononiensis* intermediate morphotypes.

The second group of Pliocene sedimentary units (7c and 7d, Fig. 23.7; 3.30–2.50 Ma interval, Fig. 23.5) consists of a fining-upward succession of fan-delta deposits capped by prodelta and open-

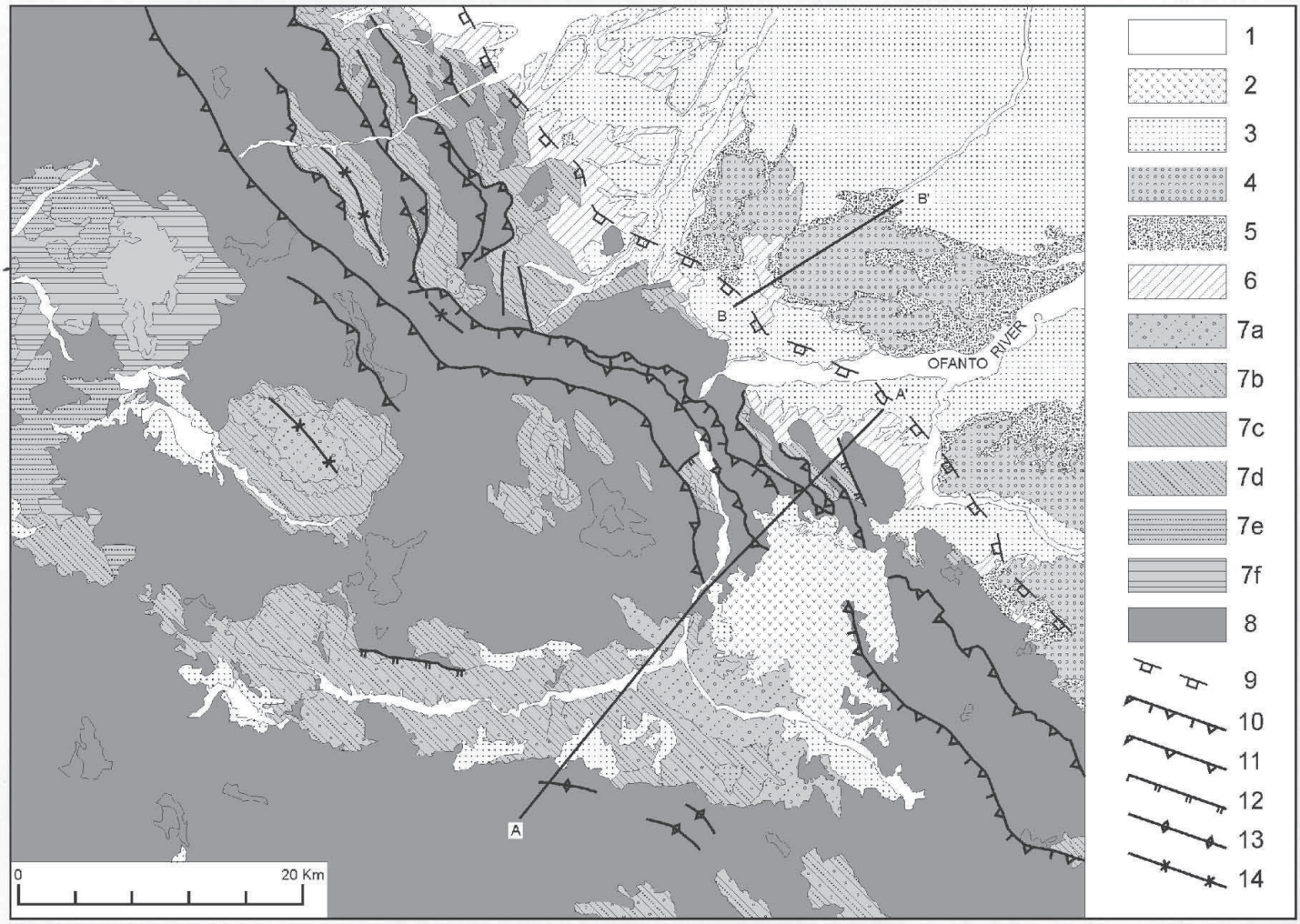

Figure 23.7 Schematic geological map showing the distribution of the upper Pliocene to Pleistocene deposits and the major structural features in the Ofanto–Vulture region (northern transect) (A–A' and B–B' are the traces of the northern composite cross section of Figure 23.9; 1, alluvial deposits (Holocene); 2, volcanites and volcanoclastic deposits (Middle Pleistocene); 3, terraced continental deposits (Middle–Upper Pleistocene); 4, prograding fluvio-deltaic deposits (Irsina Conglomerate, Middle Pleistocene); 5, shallow-marine deposits (Monte Marano Sandstone, Middle Pleistocene); 6, $Q_{1\text{-}2}$ depositional sequence: shelf mudstones (Sub-Apenninic Clay, Lower–Middle Pleistocene); 7, $P_{1\text{-}2}$ depositional sequence: 7a, prograding fan-delta conglomerates and conglomeratic sandstones (upper Pliocene); 7b, fan-delta deposits and shallow-marine sandstones (upper Pliocene); 7c, prodelta to open-shelf mudstones (upper Pliocene); 7d, fan-delta conglomerates and (outer margin of the thrust belt) shallow-marine bioclastic sandstones and silicoclastic calcarenites (upper Pliocene); 7e, shallow-marine sandstones (upper Pliocene); 7f, open-shelf mudstones (lower–upper Pliocene); 8, Apenninic nappes and thrust-sheet-top deposits older than 3.70 Ma; 9, buried front of the Apenninic nappes; 10 and 11, Pliocene and Lower–Middle Pleistocene thrusts (10, Stigliano ramp); 12, normal fault; 13, anticline axis; 14, syncline axis).

shelf mudstones. These deposits form a deepening-upward sequence that crops out discontinuously along the margins of the Ofanto synform and in an axial culmination of the synform (Fig. 23.7). The proximal fan-delta deposits are represented by massive, amalgamated and matrix-supported, red alluvial conglomerates (Paternopoli, Monticchio railway station). These deposits laterally grade toward the N and NE (Andretta, Lacedonia, Aquilonia) into well-bedded channelized fan-delta–plain conglomerates intercalated with sporadic palustrine sandy clays (distal fan-delta), and finally into delta front sandstones and pebbly sandstones along the southern margin of the Trevico syncline (few kilometres north of the Ofanto synform, Fig. 23.7). Marine clays and silty clays represent the overlying prodelta deposits. In the lower portion, these deposits contain (Monticchio railway station) a thin, discontinuous volcanoclastic layer (approximately 2.89 Ma according to our calibration) associated with spicule-rich diatomitic clays. The rich and diversified foraminiferal association is characterized by *Globorotalia bononiensis*, dextral and sinistral *Globorotalia crassaformis*, *Gt. puncticulata–Gt. bononiensis* transitional morphotypes and *Gt. aemiliana* (Spaak's VIa foraminiferal zone) together with *Planorbulina mediterranensis, Bulimina inflata, Bulimina fusiformis* and *Bulimina basispinosa*. The nannofossils record the time span between the upper part of the NN16a zone in correspondence to the temporary absence of *D. tamalis* and the lowermost part of the NN18 zone. Landward, along the western margin of the Ofanto synform, the marine mudstones grade into dark-coloured clays and silty clays, which yield a benthic foraminiferal association (*Ammonia, Elphidium* and *Florilus boueanum*) indicative of a shallow, brackish-water environment and restricted circulation. In seismic profiles, the muddy interval (2.99–2.50 Ma, Fig. 23.10a) exhibits a nearly reflection-free configuration, and is laterally substituted toward the NE by subparallel to divergent weak reflectors overlain and underlain by packages of stronger reflectors.

The above described upper Pliocene muddy sediments are abruptly overlain by a thick pile of cyclically stacked fan-delta deposits (7b, Fig. 23.7) forming a wedge-shaped sedimentary body characterized by the widespread occurrence of growth strata; that is, of syntectonic sediments with internal stratal architecture that records the progressive growth of folds in the hangingwall of active thrusts. Growth strata display progressive internal unconformities (progressive unconformity, or intraformational unconformity; Riba, 1976). These fan-delta deposits show evidence of wave and storm activity; they are organized into (1) a fining-upward lower sequence ending with a marine-flooding episode, and (2) a coarsening-upward upper sequence. The maximum flooding is testified by a few tens of metres of silty mudstones that yield sporadic *Globorotalia inflata* and nannofossil associations indicative of the NN18 zone.

The fan-delta deposits of the Ofanto synform younger than 2.50 Ma are seismically imaged by relatively continuous offlapping reflectors alternating with reflection-free zones. The line drawing of Figure 23.10a shows the overall wedge-shaped geometry of this sedimentary body, delimited by a diachronous basal unconformity and internally characterized by several progressive unconformities. We have interpreted this unit as the filling of a satellite basin located in front of the upper Pliocene leading edge of the Apenninic duplex system. The geometry of the progressive unconformities provides evidence of an early backward (southward) tilt of the basin between 2.50 and 2.13 Ma. This tilt was related to a breach emanating from the leading edge of the duplex system, which cut across the pile of nappes forming the thrust toe. A subsequent tilt toward the north was caused by the final growth of the San Fele antiformal stack. The normal fault displacing the 3.70–2.50 Ma thrust-sheet-top deposits and gently deforming the Pliocene sediments younger than 2.50 Ma may be considered as providing accommodation in the backlimb of the ramp-anticline which developed in the hanging wall of the active ramp (Fig. 23.9)

Along the northeastern margin of the Ofanto synform, the above described fan-delta systems are overlain by a new prograding unit (7a, Fig. 23.7) composed of very coarse-grained fan-delta conglomerates and conglomeratic sandstones. The occurrence of *Bulimina elegans marginata* in thin clayey interbeds within the lower portion of

the unit places this sudden and significant progradational event in the uppermost part of the Spaak's IX foraminiferal zone, close to the Pliocene–Pleistocene boundary. Younger (Lower Pleistocene?) thrust-sheet-top deposits are represented in the area by red fluvial conglomerates unconformably overlying the above-described Pliocene deltaic deposits. Due to the scale, these small outcrops have not been mapped in Figure 23.7.

Northeast of the Ofanto synform, the section cuts across several Pliocene–Pleistocene imbricates, the most continuous one being represented by the hangingwall of the Stigliano ramp (Figs 23.7, 23.9). Upper Pliocene thrust-sheet-top deposits involved in the imbricate structures are poorly represented along the trace of the profile, but are widespread and quite well exposed in the region. These Pliocene deposits display different facies architecture from those of the Ofanto synform, being characterized by a complete and apparently gradational transgressive–regressive sequence. The transgressive portion (3.30–2.99 Ma interval, Fig. 23.5) is represented by marine-bar deposits that unconformably overlie the allochthonous sheets. Discontinuous, irregular pebble-lag layers locally mark the unconformity surface. Well-sorted bioclastic sandstones and silicoclastic calcarenites typically displaying highly bioturbated foresets, frequently cut by internal erosional surfaces, characterize the marine-bar deposits. The sporadic occurrence of *B. basispinosa* in the upper part of these shallow-marine deposits is the only available significant record of a transgression that took place in the *Anomalinoides helicinus* zone. The described sandy shelf deposits grade upward, as everywhere else along the outer margin of the Southern Apennines, into open-marine clays and marly clays (2.99–2.13 Ma interval, Fig. 23.5), yielding rich and diversified foraminiferal assemblages characterized by the presence of *Gt. crassaformis*. This form co-occurs with *Gt. bononiensis* and *Gt. puncticulata–Gt. bononiensis* transitional morphotypes in the lower part of the mudstones and with *Bulimina marginata* and *Gt. bononiensis–Gt. inflata* transitional morphotypes in the upper part. The nannofossils are representative of the interval between the NN16a zone (below the temporary absence of *D. tamalis*) and the NN18 zone (just above the increase of *Discoaster triradiatus*). Unlike the Ofanto synform, where a sudden change from prodelta mudstones to delta-front sandstones and conglomeratic sandstones took place around 2.50 Ma, in the external Apenninic areas the open-shelf pelitic deposits extended upwards until

Figure 23.8 (*opposite page*) Schematic geological map showing the distribution of the upper Pliocene–Pleistocene deposits and the major structural features in the Sant'Arcangelo–Matera region (southern transect) (C–C', D–D', E–E' and F–F' are the trace of the southern composite cross section of Figure 23.9. G–G' shows the trace of the intermediate cross section of Figure 23.12; 1, alluvial and subordinate shore deposits (Holocene); 2, terraced continental and shallow-marine deposits (Middle–Upper Pleistocene); 3, alluvial and prograding fluvio-deltaic deposits (Serra Corneta Conglomerate in the Sant'Arcangelo synform, Irsina Conglomerate in the Bradano trough, Middle Pleistocene); 4, shallow-marine to backshore deposits (Monte Marano and Staturo sandstones, Middle Pleistocene); 5, Q_{1-2} depositional sequence: 5a, alluvial deposits in the Sant'Arcangelo synform (Castronuovo Conglomerate, Middle Pleistocene); slope-type fan-delta deposits along the outer margin of the Apennines north of the Nocara ridge ("Serra del Cedro Upper Conglomerate", Middle Pleistocene); 5b, lacustrine deposits (San Lorenzo clay, Middle Pleistocene); 5c, fan-delta deposits, including proximal alluvial fans (Sinni Synthem, Lower–Middle Pleistocene); 5d, prodelta mudstones and subordinate brackish-water lagoonal deposits in the Sant'Arcangelo synform (upper portion of the Sarmento Synthem, Lower Pleistocene); nearshore (Montalbano Sandstone, Middle Pleistocene) and open-shelf deposits (Gravina clays, Middle Pleistocene; Sub-Apenninic Clay, Lower–Middle Pleistocene) in the Bradano trough; 5e, deepening-upward carbonate-ramp deposits (Gravina Calcarenite, Lower–Middle Pleistocene); 5f, fan-delta to shelf deposits (lower portion of the Sarmento Synthem; Tursi Sandstone along the eastern margin of the Nocara ridge; "Serra del Cedro Lower Conglomerate" along the Apenninic margin north of the Nocara ridge, Lower Pleistocene); 5g, chaotic slope deposits (Lower Pleistocene) in the footwall of the nappe frontal ramp (Basento Valley); 5h, shallow-marine sandstones (Sant'Arcangelo and Garaguso sandstones, Lower Pleistocene); 5i, shelf mudstones (Craco Clay, Lower Pleistocene); 6, P_{1-2} depositional sequence: fan-delta-front to shallow-marine conglomerates and sandstones, lagoon to open-shelf mudstones including subordinate diatomitic clays, fan-delta-front conglomerates and sandstones laterally grading (outer margin of the Apennines) into bioclastic sandstones and silicoclastic calcarenites (upper Pliocene); 7, Apenninic nappes and thrust-sheet-top deposits older than 3.70 Ma; 8, Mesozoic carbonates of the Apulia foreland; 9, front of the Apenninic nappes; 10 and 11, Pliocene and Lower–Middle Pleistocene thrusts (10, Stigliano ramp); 12, normal fault; 13, strike-slip fault; 14, anticline axis; 15, syncline axis).

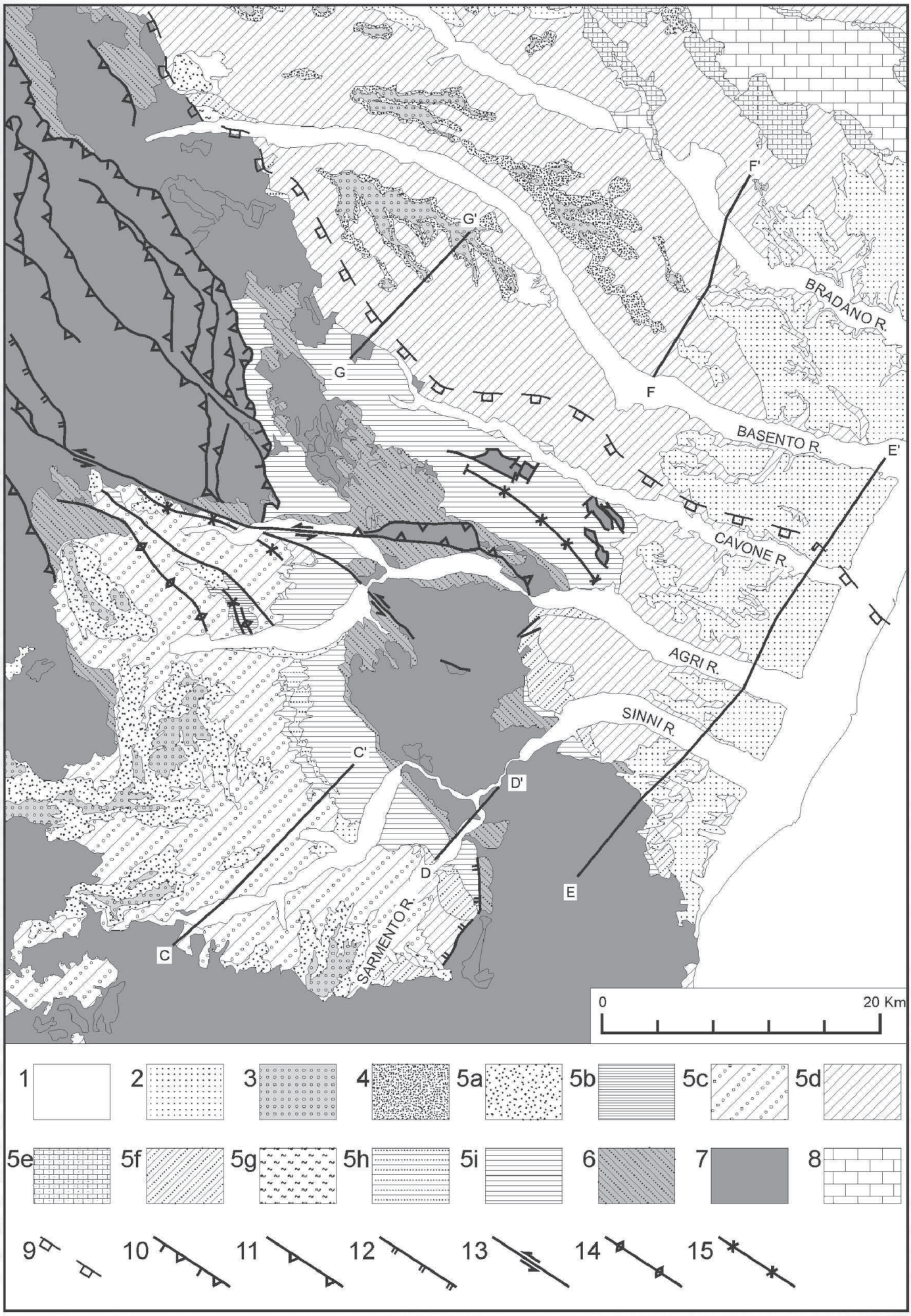
F'
G'
BRADANO R.
G
F
BASENTO R.
E'
CAVONE R.
AGRI R.
SINNI R.
C'
D'
D
E
C
SARMENTO R.
0
20 Km
1
2
3
4
5a
5b
5c
5d
5e
5f
5g
5h
5i
6
7
8
9
10
11
12
13
14
15

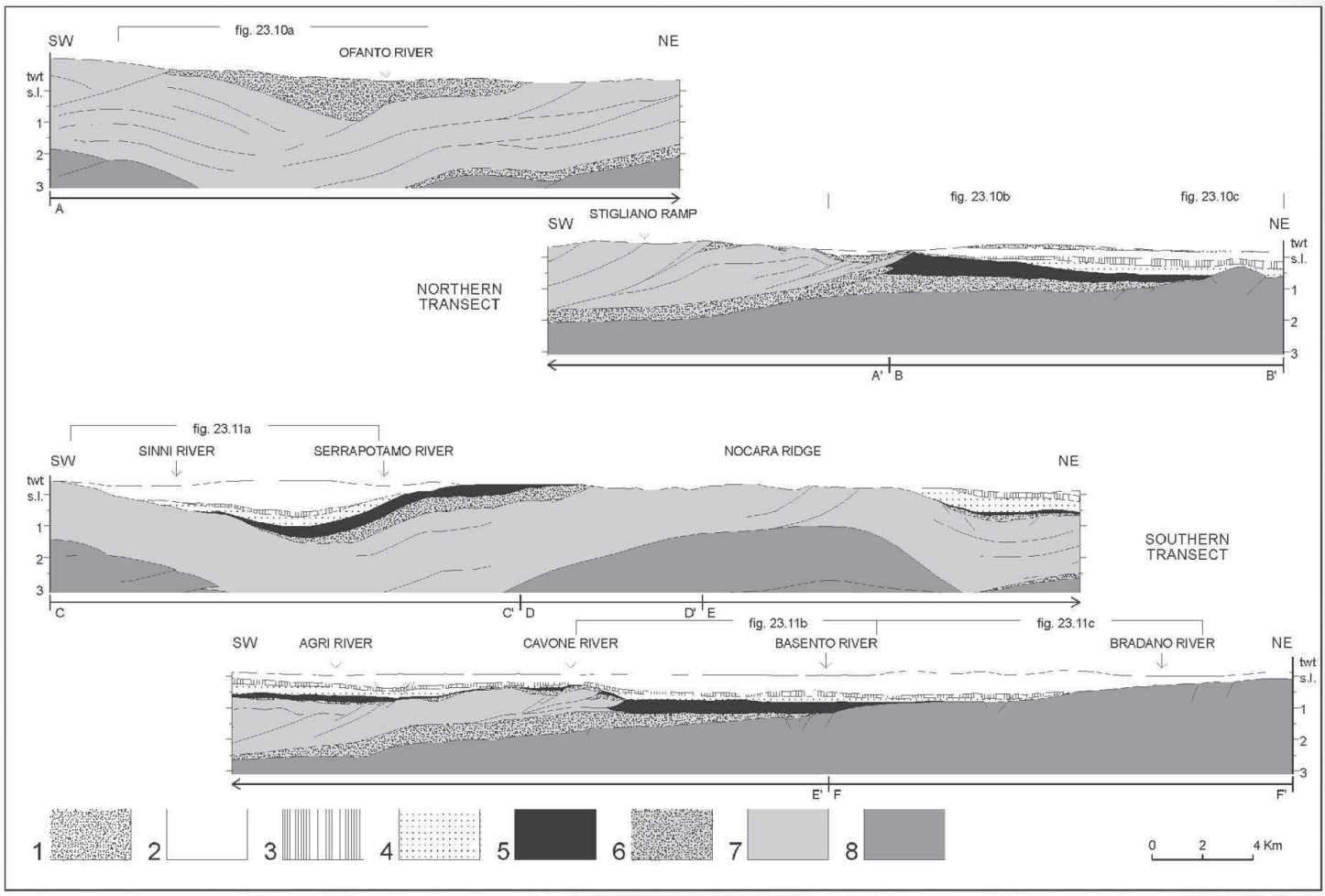

Figure 23.9 Composite cross sections along the northern (A–A', B–B') and southern (C–C', D–D', E–E' and F–F') transects (see locations in Figures 23.7 and 23.8 respectively). Vertical scale in seconds (TWT below sea level). Thin veneers of continental to shallow-marine unconformable Middle–Upper Pleistocene deposits (Figs. 23.7, 23.8) have not been included: 1, Irsina Conglomerate, Monte Marano and Staturo sandstones; 2, $Q_{1\text{-}2}$ depositional sequence, 0.92–0.66 Ma interval: fan-delta deposits of the Sinni Synthem, Montalbano Sandstone, upper portion of the Sub-Apenninic Clay (including the Gravina clays) and Gravina Calcarenite; 3, $Q_{1\text{-}2}$ depositional sequence, 1.25–0.92 Ma interval: clayey upper portion of the Sarmento Synthem and lower portion of the Sub-Apenninic Clay; 4, $Q_{1\text{-}2}$ depositional sequence, 1.50–1.25 Ma interval: sandy and pebbly deposits of the lower portion of the Sarmento Synthem, Tursi Sandstone and time-equivalent deposits in the foredeep basin; 5, $Q_{1\text{-}2}$ depositional sequence, 1.83–1.50 Ma interval: Craco Clay and Sant'Arcangelo Sandstone on top of the Apenninic nappes, prograding slope-fan deposits in the foredeep basin; 6, foredeep and thrust-sheet-top deposits of the $P_{1\text{-}2}$ depositional sequence; 7, Apenninic nappes; 8, Apulia carbonates).

about 2.13 Ma, forming a sheet some hundreds of metres thick overlain by shallowing-upward inner-shelf sandstones and pebbly sandstones (Lacedonia, Sant'Agata, Acerenza). The fossil content of the upper portion of the mudstones is usually represented by long-ranging late Pliocene taxa, but the sporadic occurrence of *Brizalina alata* in the overlying sandstones suggests that the regressive episode in the external Apenninic areas took place within the *Gt. inflata* zone. Along the whole Apenninic margin the described Pliocene deposits are unconformably overlain by Lower Pleistocene shelf mudstones (Sub-Apenninic Clay, unit 8, Fig. 23.7) yielding sporadic *Hyalinea baltica* (Montcharmont Zei, 1955).

The northeastern portion of the cross-section in Figure 23.9 shows the geometric configuration and the major tectonic and stratigraphic features of the Apenninic margin and the adjacent foredeep basin. The autochthonous carbonates of the Apulia platform, together with overlying discontinuous Messinian evaporites and post-evaporitic brackish-water mudstones, form a sort of homocline gently dipping toward the SW. The Apenninic front is represented, as in the whole northern segment of the Lucania Apenninic margin, by a

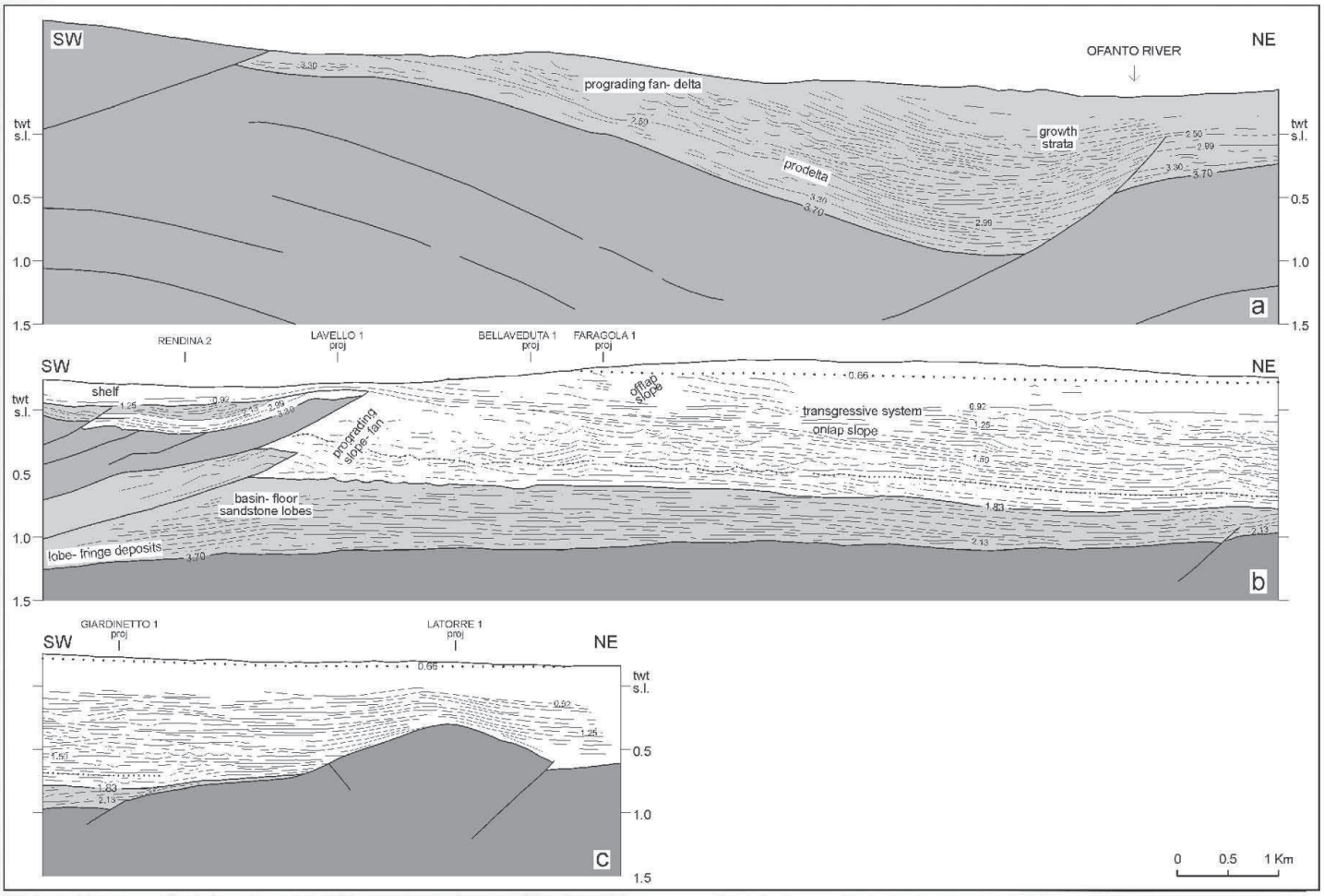

Figure 23.10 Line drawings across selected segments of the northern transect (Fig. 23.9): A. Stratigraphic interpretation of the Pliocene thrust-sheet-top deposits filling the Ofanto synform (vertical scale in seconds (twt below sea level); B, C. Stratigraphic interpretation of the Pliocene–Pleistocene deposits filling the foredeep basin in the Vulture region (seismic line provided by Edison Gas; vertical scale in seconds (twt below sea level).

steep frontal ramp where the vertical displacement exceeds 1000 m.

The Pliocene–Pleistocene deposits filling the foredeep basin have been divided into several units on the basis of an integrated interpretation of well-log curves, seismic facies and biostratigraphic data (Fig. 23.10b). The thin 3.70–2.13 Ma Pliocene interval includes two facies units. (1) The lower unit, correlated with the previously described 3.70–3.30 Ma mudstone–sandstone couplet unconformably draping the allochthonous sheets, is here represented by a nearly continuous veneer of foraminiferal limestones and marls yielding *Gt. puncticulata* and *U. rutila*. The upper unit (3.30–2.13 Ma interval), temporally corresponding to the bulk of the clastic sedimentation in the Ofanto synform, is represented in the foredeep basin by a stack of very thin-bedded turbidite sandstones and mudstones (Lavello 1 between 1449 and approximately 1915 m). These laterally grade into muddy deposits yielding *Globorotalia* gr. *crassaformis* (Bellaveduta 1 between 1550 and 1812 m; Calvino 1 between 1547 and 1733 m). These low-density turbidites, interpreted as lobe-fringe deposits, are seismically characterized by a package of highly continuous parallel reflectors with low frequency and moderate amplitude, grading toward the foreland into a reflection-free zone. A calcarenite layer, marked in the well-logs by a shift of the resistivity curve (Lavello 1 at 1670 m, Bellaveduta 1 at 1711 m, Calvino 1 at 1730 m, Maschito 1 at 1952 m, Rendina 1 at 1554 m) and seismically expressed by a strong and continuous flat reflector, constitutes a widespread and readily identifiable key bed useful for subsurface correlation in the whole area. In proximity of the nappe front, the calcarenite key bed separates a lower portion consisting of a thinning-upward

stack of muddy turbidites from an upper portion made up of relatively sand-rich turbidites organized into an overall thickening-upward succession (Lavello 1). The calcarenite key bed possibly corresponds to the maximum starvation episode recognized in the thrust-sheet-top deposits between 2.80 and 2.50 Ma (Fig. 23.5).

A thick pile of upper Pliocene turbidites showing a very high sand/mud ratio overlies the lobe-fringe deposits. These turbidites are commonly characterized in well logs by a broadly serrated cylinder-shaped profile locally interrupted by high-resistive, thin, conglomeratic layers (Lavello 1 between 1000 and 1449 m, Bellaveduta 1 between 1090 and 1550 m, Faragola 1 between 1250 and 1530 m, Giardinetto 1 between 965 and 1045 m, Maschito 1 between 1730 and 1820 m). In seismic profiles, these deposits are expressed by relatively continuous strong reflectors with even-parallel to gently mounded configurations, the latter displaying very subtle bi-directional downlap terminations. They are interpreted as aggradational to slightly progradational basin-floor lobes. Toward the foreland, downlapping reflectors tilted backward (southwestward) and truncated by the overlying clastic wedge (Fig. 23.10c), together with episodes of synsedimentary faulting and slumping (Fig. 23.10b), show active flexure-hinge retreat.

A broadly wedge-shaped sedimentary body represents the most prominent depositional feature of the foredeep basin. The sedimentary body has a thickness of about 1000 m and a width of 15 km (unit 5, Fig. 23.9). It is made up of prograding, dominantly channelized slope-fan deposits accumulated during Santernian times on the footwall of the active frontal ramp, fed by a sustained sediment supply from the uprising hangingwall (synramp deposits, 1.83–1.50 Ma interval, Fig. 23.10b,c). The base of this thrust-related slope-fan system is imaged by a very strong continuous reflector (Fig. 23.10b), which corresponds to an episode of prolonged sediment starvation (condensed section, Fig. 23.5), and represents a first-order unconformity surface on top of the underlying seismic unit. The clastic wedge consists of two major prograding slope-fan units (separated by a dotted line in Figure 23.10b) internally organized into three basic architectural elements. The stratal geometry is particularly evident in the upper slope-fan unit. The updip (proximal) portion basically consists of mass-transported muddy deposits derived from the uprising allochthonous sheets. These deposits imaged by contorted to chaotic seismic facies, locally show well defined, concave-upward, strong reflectors interpreted as large intraformational erosional features. Well-logs show random distribution of the dipmeter data and linear shaly SP (self potential) profiles, except in correspondence to highly resistive channel-fill conglomerates and to more competent lithologies interpreted as slides derived from the Apenninic nappes (Lavello 1 between 426 and 1000 m, Bellaveduta 1 between 630 and 1090 m, Calvino 1 between 975 and 1355 m, Maschito 1 between 640 and 1730 m). The chaotic and massive deposits grade downdip, with evident large-scale offlapping geometry, into a channel-overbank system seismically typified by a network of irregular and discontinuous strong reflectors with negative relief. Towards the basin, the channel-overbank deposits rapidly pass into a sheet of well-bedded sandy turbidites characterized by irregular blocky well-log profiles (Giardinetto 1 between 760 and 965 m) and seismically indicated by moderate to high amplitude, continuous subparallel reflectors which progressively onlap the outer (northeastern) margin of the foredeep basin (Fig. 23.10c).

Pliocene deposits with depositional features similar to those characterizing the Santernian synramp deposits in the Lucania Apennine have been described in the Torrente Tona oil-field area, about 50 km north of our study region (Rossi, 1986).

During the growth of the Apennine frontal structures no significant tectonic activity seems to have affected the foreland "homocline". The forward-onlapping stratal pattern of the Santernian turbidites points to a confined foredeep basin in the absence of significant addition of accommodation space by active faulting or flexure retreat. The only indication of tectonic instability is given by the sporadic occurrence of slumps, seismically manifested by weak chaotic responses.

The offlapping clastic wedge directly fed by the hangingwall of the active frontal ramp and secondarily by submarine valley systems (longitudinally-dispersed channel-fill conglomerates), is overlain by a mixed sand–mud onlap-slope system

(1.5–1.25 Ma interval, Figs 23.5, 23.10b,c). Updip, the latter is composed of thin, discontinuous and irregular layers of sandy turbidites characterized by spiky SP profiles in well logs (Giardinetto 1 between 514 and 760 m). Discontinuous subparallel weak reflectors seismically express these sands. In seismic sections, the base-of-slope deposits pass downdip into a network of discontinuous concave reflectors forming a complex backstepping array of channel-fill deposits. This facies grades into more distal thin sandy turbidites and hemipelagic clays (La Torre 1 between 345 and 400 m) which onlap and drape a local structural high. The onlap-slope system records a destructional slope, laps landward over weakly eroded portions of the synramp clastic wedge, and is overlain by transgressive muddy deposits (1.25–0.92 Ma interval, Figs 23.5, 23.10b,c). Updip, the latter unconformably drape the allochthonous sheets, suturing the frontal ramp. This transgressive unit, the base of which is commonly marked on well-logs by shaly SP and resistivity response (Giardinetto 1 between 494 and 514 m), is seismically characterized by retrogressive subtle sigmoid clinoforms laterally passing into weak reflectors with widespread chaotic configuration. This indicates extensive slope failures and sediment remobilization by slump processes. In correspondence to Giardinetto 1 (Fig. 23.10c), continuous, wavy reflectors indicate bottom-current-reworked sands. In well logs these sands have a sharp-based bell-shaped SP curve. Toward the basin floor, very fine-grained turbidite deposits, featured by spiky well-log profiles with an overall thickening-upward characteristic and by subparallel continuous seismic reflections, form well-organized sheet lobes.

The onlap stratal pattern of the 1.50–1.25 Ma interval and the transgressive characteristic of the 1.25–0.92 Ma deposits on top of the allochthonous sheets testify the deactivation of the Apenninic frontal ramp around 1.50 Ma. The deactivation coincided with the establishment of a passive destructional retrograding margin followed by a short-lived depositional slope indicative of a very low sediment supply from the adjacent shelf. The decrease in volume and grain size of the sediments in the basin during the 1.50–0.92 Ma interval points to a progressive reduction of the alluvial gradients in the feeder system. This is in agreement with the increase in the accommodation space on the shelf testified by transgressive deposits. A forward thrust propagation after the deactivation of the frontal ramp might be suggested by the growth of a fold in correspondence to the La Torre 1 structural high (Fig. 23.10c). However, the La Torre pop-up-like structure may be better interpreted as a synsedimentary transpressive feature created by strike-slip faults active in the foreland region, rather than as a fold related to a forward propagation of the sole thrust.

The 1.25–0.92 Ma transgressive system is overlain by an overall reflection-free muddy unit (0.92–0.66 Ma interval), which only locally shows discontinuous weak reflectors with sigmoid-oblique configurations providing evidence of a high-energy offlap-slope system. The prograding shelf-margin indicates a renewed clastic supply from the adjacent shelf. Nevertheless, the persistent muddy characteristic of the prograding slope points to a feeder system having a low topographic relief with large tracts dominated by fine-grained suspended load.

Younger Quaternary sediments cut across by the section, but having no record in the seismic line, are represented by shelf mudstones vertically evolving into a prograding sandy barrier-system which is in turn overlain by coarse-grained fluvio-deltaic deposits (Monte Marano Sandstone and Irsina Conglomerate, units 5 and 4 of Fig. 23.7 respectively). The base of this unit, marked by a dotted line in Figures 23.10b and c (0.66 Ma isochron), was obtained by projecting onto the line drawing the available surface information.

A problem of the northern transect is the nature and provenance of the lower imbricate forming the Apennine frontal thrust system. The Rendina 2 well, located about 2 Km behind the nappe front (Fig. 23.10b), has penetrated about 500 m of Pleistocene–Pliocene thrust-sheet-top deposits and about 400 m of allochthonous sheets. Below the allochthonous sheets, from 892 to 1321 m (total depth), the borehole penetrated Pliocene deposits displaying a well-log profile correlatable with the profiles of the sandy-lobe and lobe-fringe deposits, including the calcarenite key bed, which lie above the autochthonous Apulia carbonates. Whatever realistic velocity values are assigned to

the Pliocene–Pleistocene foredeep deposits, and considering that the calcarenite key bed was found at 1670 m depth in Lavello 1 it is clear from Figure 23.10b that the Pliocene units below the allochthonous sheets in Rendina 2 lie at shallower depths than the coeval autochthonous foredeep deposits. Consequently, the 892–1321 m Pliocene interval of Rendina 2 is part of the frontal imbricate system. We must conclude that before the development of the frontal ramp, the sole thrust in front of the duplex leading edge had to deepen from the base of the Apenninic nappes to the interface between the autochthonous Mesozoic–Tertiary Apulia carbonates and the overlying Pliocene foredeep deposits. In such a way portions of Pliocene foredeep deposits were detached from the original substratum and incorporated in the tectonic wedge.

Southern transect

The southern transect extends from the western margin of the Sant'Arcangelo synform (foot of the Apennine duplex system) to the Apulia foreland in correspondence to the Matera high (Figs 23.2, 23.8). The transect cuts across the Sant'Arcangelo synform, the Nocara ridge, the buried front of the Apenninic nappes and the foredeep basin (Figs 23.9, 23.11). Along this transect the almost continuous sedimentary record on top of the thrust sheets and the numerous biostratigraphic constraints allowed the identification of well-tied isochronous sedimentary units showing remarkable lateral variations of facies.

The Sant'Arcangelo synform usually has been described as a Pliocene–Pleistocene satellite basin formed on top of the allochthonous sheets during the Apennine compression. According to Caldara *et al.* (1988) and Pieri *et al.* (1994) the basin evolution was characterized by a progressive forward (northeastward) migration of the depocentre; according to Hippolyte *et al.* (1991), Hippolyte (1992), Camarlinghi (1992) and Hippolyte *et al.* (1994b), by contrast, the depocentre migrated from NE to SW because of a syndepositional tilt caused by the growth of the Nocara ridge. The stratigraphic reconstruction of Caldara *et al.* (1988) and Pieri *et al.* (1994) has been criticized by Zavala and Mutti (1996) who proposed a new depositional model based on an extensive sedimentological investigation (Mutti, E. *et al.*, 1996; Zavala and Mutti, 1996). However, because of the lack of sufficient biostratigraphic data, these authors have correlated sedimentary units of different ages; so that some assumed lateral changes of facies refer instead to characteristics of sedimentary units deposited in different times and tectonic settings. One example is the so called Tursi "Allogroup" (defined by Zavala and Mutti, 1996), in which proximal, poorly organized conglomerates widespread in the Armento Stream, Sauro River and Alianello areas (Sant'Arcangelo synform) have been correlated with shelf sandstone lobes (Tursi Sandstone) developed along the eastern margin of the Nocara ridge. The Tursi Sandstone contains *H. baltica* associated with large *Gephyrocapsa* spp., and belongs to the NN19d nannofossil zone, and is older than 1.24 Ma. In contrast, the coarse-grained deposits of the Sant'Arcangelo synform included by these authors in the Tursi "Allogroup", stratigraphically overlie prodelta mudstones belonging to the NN19f nannofossil zone and consequently are younger than 0.94 Ma (Marino, 1993, 1996b).

Our reconstruction of the Sant'Arcangelo area agrees with those of Camarlinghi (1992), Hippolyte (1992) and Hippolyte *et al.* (1994b) for the overall geometry of the Pliocene–Pleistocene deposits filling the synform, but differs somewhat in the times and modes of the deformation. Useful contributions to our reconstruction have been provided by the detailed geological maps of the northern part of the area edited by Lentini (1991) and by the accurate facies analysis of the Pleistocene sedimentary units by Caldara *et al.* (1988).

The Pliocene deposits (Caliandro cycle, in Vezzani, 1967; Pieri *et al.*, 1994; Catarozzo Group, in Zavala and Mutti, 1996; $P_{1\text{-}2}$ thrust-related depositional sequence in this chapter) are well exposed along the northwestern, northern and eastern margins of the Sant'Arcangelo synform (unit 6 in Fig. 23.8; 3.30–1.83 Ma interval in Fig. 23.6). The transgressive lower portion is represented by disorganized matrix-supported fan-delta-front conglomerates (proximal cohesive debris-flow deposits) grading in the northwestern flank of the Nocara ridge into more distal coarse-grained sandy turbidites (gravity-flow deposits laid down in front of distributary channels) and

into dark-coloured brackish-water lagoonal mudstones. These deposits grade vertically (northwestern margin of the Sant'Arcangelo synform) and laterally (northern and eastern flanks of the Nocara ridge) into well-sorted bioclastic sandstones and silicoclastic calcarenites (marine bars) showing large, low-angle, tabular cross-stratification, shell lags and frequent reactivation surfaces locally obscured by highly pervasive bioturbation. A widespread diachronous clayey unit temporally tied by several biostratigraphic constraints overlies the fan-delta-front and the marine-bar deposits. This unit is largely composed of prodelta mudstones which grade westward into brackish-water lagoonal deposits (northwestern flank of the Sant'Arcangelo synform) and eastward into open-shelf foraminiferal mudstones. All around the Nocara ridge, the lower part of the clayey unit consists of spicule-rich diatomitic clays locally including a thin discontinuous volcanoclastic layer (eastern margin of the Sant'Arcangelo synform). The base of the diatomitic clays is stratigraphically well-constrained by the occurrence of dextral and sinistral *Gt. crassaformis* associated with *Gt. puncticulata–Gt. bononiensis* intermediate morphotypes (Spaak's VIa foraminiferal zone) and by a nannofossil association indicative of the upper part of the NN16a zone in correspondence to the temporary absence of *D. tamalis*. The top of the diatomitic clays is temporally defined by the co-occurrence of sinistral *Gt. crassaformis* and *Gt. bononiensis–Gt. inflata* transitional forms indicative of the Spaak's VIb zone, and by a nannofossil assemblage still indicative of the NN16a zone but above the temporary absence of *D. tamalis*. In the northwestern flank of the Sant'Arcangelo synform, lagoon/prodelta mudstones yielding the same fossil associations directly overlie shallow-marine sandstones without interposed diatomitic clays (Fig. 23.6). These stratigraphic relations clearly testify to a landward transition of the diatomitic clays into the shallow-marine sandstones. In the same area, the top of the prodelta mudstones is temporally fixed by the occurrence of *B. marginata* associated with an increasing abundance of *Neogloboquadrina atlantica* in the foraminiferal assemblage and by the disappearance of *Discoaster surculus* and *Discoaster pentaradiatus* in the nannofossil association (base of the NN18 nannofossil zone tuned to the Spaak's VII foraminiferal zone). Still along the northwestern margin of the synform, the described mudstones are overlain by regressive, shallowing-upward fan-delta-front sandstones and conglomeratic sandstones where the common occurrence of pebble imbrication testifies widespread wave reworking.

Along the eastern margin of the Sant'Arcangelo synform and in correspondence to the northern termination of the Nocara ridge, the prodelta clayey unit grades upwards into about ten metres of storm-reworked shallow-marine sandstones and sandy clays. The uppermost part of the prodelta mudstones is temporally tied by an increase of *D. triradiatus* in the nannoflora and by the first occurrence of *Gt. inflata* in the foraminiferal association (Marino, 1993, 1994). The first appearance of *Globorotalia truncatulinoides* immediately followed by the disappearance of *Discoaster broweri* and *D. triradiatus* in the nannoflora were recorded in clayey interbeds of the regressive sandier interval. These biostratigraphic data imply a lateral transition between the regressive fan-delta-front sandstones of the western outcrops and the upper portion of the prodelta clayey sequence in the eastern outcrops.

Along the transect, the described Pliocene deposits are exposed only in the eastern flank of the Sant'Arcangelo synform, but they extend in the subsurface toward the SW as far as the centre of the depression (unit 6 in the cross-section of Fig. 23.9) with a seismic facies characterized by subparallel reflectors with low to moderate amplitude and continuity which onlap against the Apenninic nappes (3.30–1.83 Ma interval of Fig. 23.11a). East of the Nocara ridge, upper Pliocene thrust-sheet-top deposits crop out discontinuously along the outer (northeastern) flank of the antiform, showing the same vertical succession of facies as in the west. These deposits have been recognized in the subsurface as far as the front of the Apenninic nappes (Fig. 23.9).

In the foredeep basin, a few metres of condensed foraminiferal limestones and marls (3.70–2.13 Ma interval in Fig. 23.11b), coeval with the transgressive portion of the described Pliocene thrust-sheet-top deposits, discontinuously drape the Apulia carbonates. The condensed deposits

are in turn overlain by a thick pile of upper Pliocene sandy turbidites containing *Gt. inflata* (2.13–1.83 Ma interval in Fig. 23.11b), which are coeval with the regressive portion of the P_{1-2} thrust-sheet-top deposits. In well-logs these redeposited sandstones are basically defined by distinctive serrated cylinder-shaped SP curves locally overlain by crescent and/or bell-shaped profiles with irregularly distributed spiky sandy packages (Andriace 1 from 1504 to 2,275 m, San Basilio 1 from about 1312 to 1978 m, Fiume Basento 1 from about 1335 to 1585 m, San Basilio 2 from about 1300 to 1552 m). In seismic profiles, reflectors having high to moderate amplitude and continuity express gently prograding mounded features with very low external relief and internal multilobate characteristic. Gently tilted downlap terminations and top-truncated reflectors testify, as in the northern transect, an episode of relevant flexure-hinge retreat just before the deposition of the overlying sedimentary unit.

In conclusion, the Pliocene thrust-sheet-top deposits cropping out in the Sant'Arcangelo area, along the outer margin of the Nocara ridge and N of this structural high form, as a whole, a transgressive–regressive sedimentary cycle. In it the general facies distribution and the absence of intraformational unconformities clearly testify to sedimentation on a wide passive shelf open toward the foredeep basin. The important turbidite accumulation in the foredeep basin during the *Gt. inflata* zone reflects the coeval fan-delta progradation in the Sant'Arcangelo synform and, in general, the regressive characteristic of the upper portion of the Pliocene thrust-sheet-top deposits of the Apenninic margin.

In the Sant'Arcangelo area and along the outer margin of the Apennines, the upper Pliocene thrust-sheet-top deposits are disconformably overlain (Fig. 23.6) by a sheet of Lower Pleistocene (Santernian) inner-shelf clays and silty clays eastward grading into open-shelf foraminiferal mudstones (Craco Clay, unit 5i in Fig. 23.8). The only available key beds in this monotonous clayey shelf unit are represented by two volcanoclastic layers, the upper one (1.64 Ma according to our calibration) probably corresponding to the well-known *m* volcanoclastic horizon of the Vrica section (Pasini and Colalongo, 1982, 1994). As for the foraminiferal content, *B. elegans marginata* dominates the assemblages from the base of the unit. Upward in the section, this form is associated with scarce *Neogloboquadrina pachyderma* left, *Globorotalia oscitans* and *Globigerina calabra*, as well as (outside the Sant'Arcangelo synform) with *Globigerina cariacoensis* and *Globigerinoides tenellus*. The nannofossil assemblages are indicative of a time interval ranging from the NN19a nannofossil zone to the NN19c zone (systematic absence of *D. broweri* in the nannoflora, presence of sporadic *Gephyrocapsa caribbeanica* just below the first occurrence of *Gephyrocapsa oceanica* with forms having an average size between 3.5 and 4 μm, disappearance of *Calcidiscus macyntirei* near the top of the clays). In the Sant'Arcangelo synform the described Santernian mudstones grade upwards into bioturbated shell-rich sandstones characterized by evident wavy bedding and internal cross-lamination (Sant'Arcangelo Sandstone, unit 5h in Fig. 23.8). Figure 23.9 shows the westward extension of the Craco Clay–Sant'Arcangelo Sandstone couplet (unit 5) along the transect. In correspondence to the eastern flank of the synform, this sedimentary couplet is seismically imaged by a nearly reflection-free unit which grades toward the SW into a package of moderate to low-amplitude, fairly continuous, subparallel to convergent reflectors showing evident onlap terminations against the Apenninic nappes (1.83–1.50 Ma interval in Fig. 23.11a). East of the Nocara ridge, the Sant'Arcangelo Sandstone is absent and is substituted by more distal muddy deposits draping the Apenninic thrust sheets as far as the nappe front.

In the foredeep basin, a prograding slope-fan system forming a relatively thick clastic wedge developed in the footwall of the active Apenninic frontal ramp during the 1.83–1.50 Ma interval (Fig. 23.11b). The slope-fan wedge unconformably overlies the above described upper Pliocene sandy turbidite lobes and rapidly thins toward the foreland with progressive onlap terminations against the outer (northeastern) margin of the foredeep basin. The lower boundary of the wedge is expressed in well logs by a pronounced positive shift of the SP curve and is seismically imaged by a flat, continuous, strong reflector, which corresponds to a significant and widespread condensed

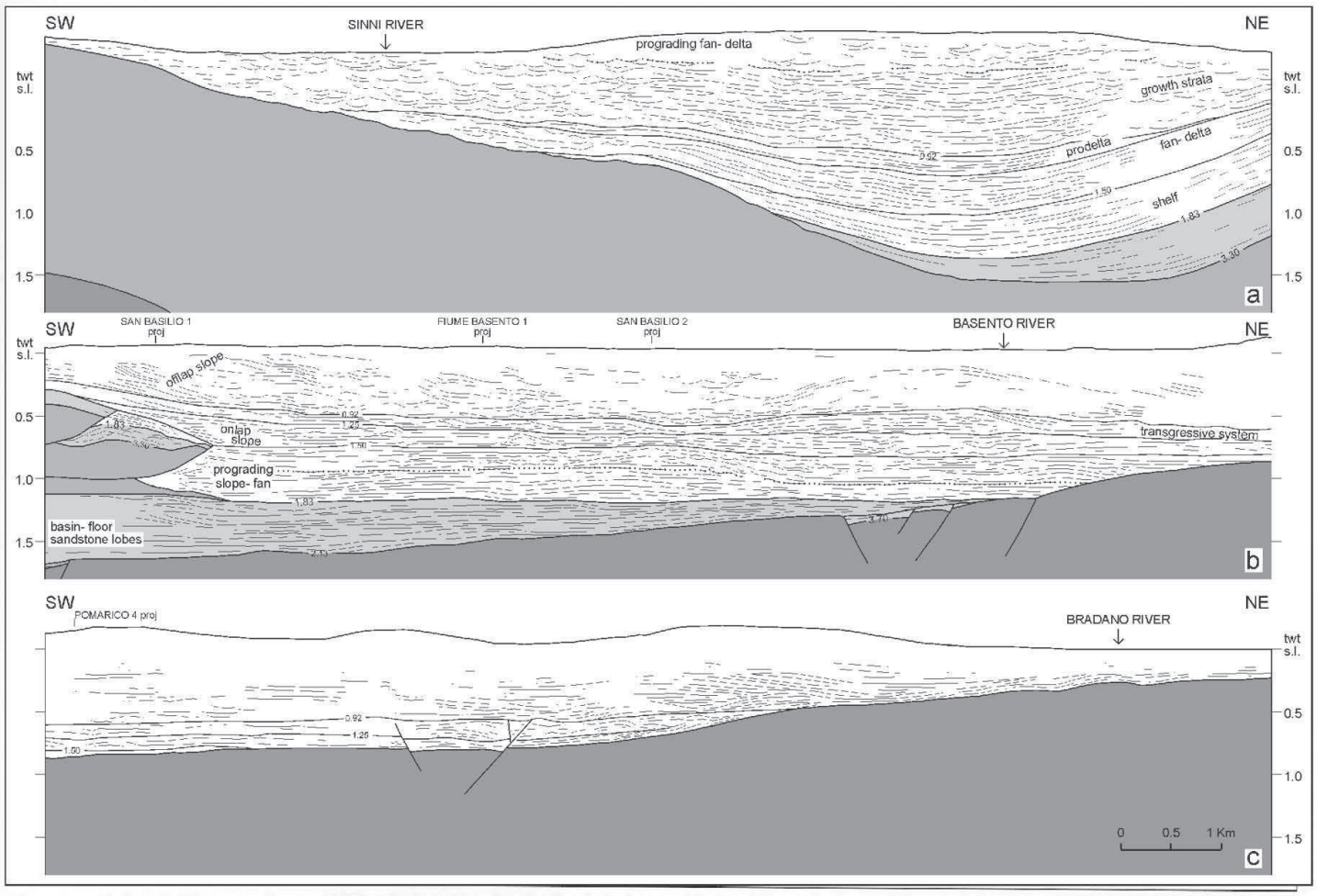

Figure 23.11 Line drawings across selected segments of the southern transect: A. Stratigraphic interpretation of the upper Pliocene to Middle Pleistocene thrust-sheet-top deposits filling the Sant'Arcangelo synform (vertical scale in seconds (twt below sea level); B, C. Stratigraphic interpretation of the Pliocene–Pleistocene deposits filling the foredeep basin in the Basento area (seismic line provided by AGIP; vertical scale in seconds (twt below sea level).

section. We have interpreted this strong signal of sediment starvation as the downdip termination by downlap of the low-energy-shelf transgressive Craco Clay. If this interpretation is correct, the foredeep slope-fan deposits very probably accumulated in a very short time interval, roughly coinciding with the shelf sedimentation of Sant'Arcangelo sandstone (1.57–1.50 Ma). The slope-fan system consists of a monotonous stack of predominantly muddy turbidites characterized by an overall spiky well-log profile which suggests irregularly distributed packages of very thin-bedded sands lacking a clearly defined stratal pattern (San Basilio 2 between 820 and 1300 m). In seismic profiles (Fig. 23.11b) the slope-fan is imaged by nearly continuous reflectors with high to moderate amplitude and frequency, displaying a quite generalized bi-directional downlapping pattern. This stratal pattern suggests an aggradational–progradational stack of discrete mounded lobes, each basinward-shifted lobe unit being top-truncated by the overlying one. This sand-poor fan-lobe system, fed and progressively truncated by the uprising hangingwall block, is arranged into two main depositional units separated by a major erosional surface seismically expressed by a very strong reflector (dotted line in Fig. 23.11b). The upper slope-fan depositional unit, better preserving the primary downfan facies distribution, consists of three main architectural elements: a well-developed inner channel-levee system characterized by nested small channels with low relief, downdip mounded depositional lobes with downcurrent external flanks modified by scours and slumps and finally a broadly parallel-layered turbidite unit having lateral pinchout geometry.

In the Sant'Arcangelo synform all the previously described upper Pliocene and Lower Pleistocene thrust-sheet-top deposits are discon-

formably overlain by backstepping, deepening-upward, clastic deposits capped by lagoon/prodelta mudstones which belong to a retrograding coarse-grained fan-delta system (Sarmento Synthem in Fig. 23.6). The lower part of this unconformity-bounded unit (Salvador, 1994) is exposed near the confluence of the Sarmento and Lappio streams and is represented by massive, amalgamated, matrix-supported red conglomerates indicative of subaerial alluvial fans (unit 5f in Fig. 23.8). These alluvial conglomerates gradually evolve vertically and laterally (toward the NE) into fan-delta-front deposits mainly represented by multi-storey channel-fill sandstones and pebbly sandstones associated with sheet-like shell lags. Near the village of San Giorgio Lucano (Sarmento Valley) the delta-front deposits grade upward into bioclastic marine bars showing large-scale cross-stratification and pervasive bioturbation. The marine bars are in turn overlain by prodelta clays and silty clays landward intertonguing with restricted, brackish-water lagoonal mudstones (unit 5d in Fig. 23.8 in the Sant'Arcangelo synform). The prodelta clays yield a poor foraminiferal association characterized by the sporadic presence of *H. baltica* and *Bulimina etnea* and relatively rich nannofossil assemblages indicative of the NN19e and NN19f zones. Figure 23.11a shows the overall backstepping stratal geometry of the Sarmento Synthem (fan-delta unit overlying the 1.50 Ma isochron), as well as the seismic configuration of the alluvial conglomerates (poorly defined and discontinuous concave-upward reflectors). The latter laterally grade into fan-delta-front deposits (hummocky to gently-mounded reflectors), which are in turn overlain by prodelta mudstones (parallel reflectors with high frequency and continuity).

Distal fan-delta-front deposits and shelf sandstone lobes, coeval with the fan-delta deposits of the Sant'Arcangelo synform, crop out east of the Nocara ridge (Tursi Sandstone, Fig. 23.6). They are represented by metre-thick sets of tabular sandstones and minor pebbly-sandstones showing a complex channel-in-channel fill pattern and by sets of hummocky cross-stratified fine to medium-grained sandstones associated with thin lenticular shell-beds and thinner sets of wave-cross-laminated fine-grained sandstones. The occurrence of granulite–amphibolite and ophiolite/metaophiolite pebbles in the coarser-grained deposits testifies to an active feeding source located in the high Sinni and Sarmento valleys. The stratal architecture of the Tursi Sandstone is well recognizable in the subsurface because of the distinctive log responses (irregular bell-shaped pattern of sandy packages, see Tursi 2 from 20 to 378 m) and the characteristic seismic expression (very high-amplitude continuous reflectors with even-parallel to gently-mounded configuration). The Tursi Sandstone disconformably overlies the Craco Clay and gradually thin toward the nappe front, smoothing topographic irregularities on top of the Apenninic thrust toe (unit 4 in Fig. 23.9). Along the northeastern flank of the Nocara ridge, the sandstones grade vertically and laterally into muddy deposits belonging to a widespread sedimentary unit known in the geological literature as the Sub-Apenninic Clay. The Tursi Sandstone is temporally confined within the 19d nannofossil zone, as indicated by the occurrence of Large *Gephyrocapsa* spp. and sporadic *H. baltica* both in the lowermost and uppermost portions of the units, as well as in the basal portion of the overlying Sub-Apenninic Clay.

In front of the nappe front, the 1.50–1.25 Ma interval consists of packages of sand-poor thin-bedded turbidites with ragged well-log profiles seismically expressed by fairly continuous subparallel reflectors with high amplitude and frequency, as well as of packages of mass-transport deposits with limited extent, seismically expressed by small sets of discontinuous to chaotic reflectors (slump scars). In the foredeep basin, large erosional channels filled with packages of fining-upward thin-bedded, ponded turbidites feature a widespread channelized system. This broadly lenticular basin-floor channel-levee system forms an intricate mosaic of laterally discontinuous facies which onlap a retrogressive slope. The latter, characterized by sediment bypass and starvation, records the deactivation of the frontal ramp. The absence of an offlapping delta-fed slope apron reflects the poor sediment supply from the adjacent shelf margin, in agreement with the confinement of the bulk of the Tursi Sandstone within topographic depressions of the shelf area (Fig. 23.9). The channelized system is substituted downdip by muddy turbidite sheet lobes which

progressively wedge out toward the foreland with an overall downlapping geometry, slightly modified by subsequent faulting and tilting (Fig. 23.11c).

Along the northeastern margin of the Nocara ridge the Tursi Sandstone is conformably overlain by open-shelf mudstones representing the lower part of the Sub-Apennine Clay unit (1.25–0.92 interval in Fig. 23.6), well exposed along the whole margin of the mountain chain. In the Sant'Arcangelo synform the previously described prodelta/lagoon deposits forming the uppermost portion of the Sarmento Synthem substitute these open-marine mudstones. The 1.25–0.92 interval of the Sub-Apenninic Clay, locally yielding *Globorotalia truncatulinoides* excelsa, is stratigraphically well-constrained by nannofossil associations which indicate a time span ranging from the top of the NN19d zone to the lowermost part of the NN19f zone (Ciaranfi *et al.*, 1996a, b; Marino, 1996a, b). In the Montalbano composite section, the lower portion of the Sub-Apenninic Clay unit includes the V_1 volcanoclastic bed and is characterized by shelf mudstones containing a relatively deep-water benthic palaeocommunity (interval I of Ciaranfi *et al.*, 1996a). In front of the Nocara ridge this interval (unit 3 in Fig. 23.9) appears as a homogeneous mud-dominated sheet continuously draping the underlying Tursi Sandstone, limited at the top by a very strong reflector and internally characterized by reflection-free facies or by packages of faint and discontinuous parallel reflectors. In correspondence to the inactive nappe front, gently dipping sigmoid reflectors indicate a low-energy depositional slope with a renewed, though modest, sediment supply from the contiguous shelf which began to act as a transfer zone for sediment transport into the foredeep basin (Fig. 23.11b). Retrogressive erosional gullies and rotational slumps in correspondence to the toe of the slope show the overall retrogradational characteristic of the system. In the basin, numerous small gullies, wide multi-storey, leveed channels and sand-dominated mounds with external downlaps partly truncated by erosional surfaces indicate that the bulk of the basin infill material was driven by currents with longitudinal dispersal related to submarine-valley systems. Weak discontinuous reflectors suggesting sheet turbidite lobes seismically image this sedimentary unit downdip. These deposits pinch out against the foreland "homocline" with an overall downlap geometry slightly modified by subsequent faulting and gentle tilting indicative of a persisting, though moderate, flexural subsidence. An irregular bumpy horizon indicates the upper boundary surface, marked by a nearly continuous strong reflector that indicates palaeobathimetric irregularities and a general sediment starvation.

The biostratigraphic constraints and the facies relations between the Sarmento Synthem and the Tursi Sandstone plus the lower interval of the Sub-Apenninic Clay clearly depict a backstepping and upward-deepening sedimentary unit developed during the 1.50–0.92 Ma interval, with maximum flooding around 0.92 Ma. This Lower Pleistocene (Emilian–Sicilian) sedimentary unit was deposited on top of the allochthonous sheets when the latter formed a passive shelf open toward the foredeep basin and extended without interruptions from the present day Sant'Arcangelo synform to the buried nappe front. Therefore, as in the case of the 3.30–1.83 Ma upper Pliocene deposits, sedimentation took place on top of an inactive thrust toe and not in a satellite basin forward limited by an active ridge as is commonly reported in the geological literature.

In the Sant'Arcangelo synform the prodelta mudstones of the Sarmento Synthem and the older Pleistocene thrust-sheet-top deposits are overlain, with progressive angular unconformity, by a thick sedimentary unit made up of coarse-grained fan-delta deposits (unit 2 in Fig. 23.9 and fan-delta deposits postdating 0.92 Ma; Fig. 23.11a) showing an evident backstepping geometry and an overall progradational facies architecture. This unit (Sinni Synthem in Fig. 23.6; unit 5c in Fig. 23.8) may be divided into two intervals, the lower one consisting of retrogradational fining-upward fan-delta deposits and the upper one of newly prograding coarsening-upward fan-delta conglomerates. The lower interval of the Sinni Synthem, well exposed along the Sinni River, is represented by coarse-grained matrix-supported alluvial conglomerates rapidly grading, toward north and northeast (Alvaro Stream, Senise), into mouth-bar deposits, made up of tabular coarse-grained sandstones with well-preserved internal foresets, and into more distal thick-bedded massive

sandstones deposited by high-density turbidity currents. Parallel-bedded conglomeratic sandstones with well-developed pebble imbrication, sporadic channel-fill conglomerates and shell lags rich in *Corbula* and *Glycimeris* are locally present. These fan-delta-front deposits interfinger landward (Cerrito and Sauro streams) with subaerial fan-delta-plain deposits mainly consisting of channel-fill sandstones and pebbly sandstones separated by overbank mudstones containing fresh-water gastropods and abundant plant roots. The boundary between the lower and the upper intervals is indicated by a dotted line on Figure 23.11a. This boundary corresponds to the maximum retrogradation of the Sinni Synthem. The facies relations observed in the field are also evident in the seismic profile where the inner alluvial-fan deposits of the lower interval, expressed by poorly-defined convex-down reflectors indicative of nested erosional channels, are laterally and vertically substituted by relatively more continuous reflectors having parallel to subtly mounded configurations indicative of marine bars in distal parts of the fan-delta system. The upper interval of the Sinni Synthem, clearly imaged in the seismic profile by discontinuous reflections with negative relief, is very well exposed along the western and northern margins of the Sant'Arcangelo synform and in the Alianello area, characterized by spectacular growth strata which give origin to a cumulative wedge-shaped sedimentary body. This coarsening-upward interval forms, as a whole, a prograding fan-delta system composed of thick, massive, red alluvial conglomerates deposited either by cohesive debris flows or by erosive highly concentrated floods. Minor tabular conglomerates locally showing pebble imbrication and internal trough cross-stratification are also present in the northern portion of the Sant'Arcangelo synform (Armento Stream, Guardia Perticara and Sauro River). Ephemeral ponds/marshes are locally indicated by black mudstones rich in *Planorbis* and plant roots interlayered with bioturbated red siltstones.

We have distinguished a Sinni Synthem and a Sarmento Synthem taking into account the remarkable angular unconformity at the base of the Sinni Synthem (indicated in Figure 23.11a by the truncation of the prodelta mudstones at the top of the Sarmento Synthem), the widespread progressive unconformities both in the lower and upper intervals of the Sinni Synthem and the occurrence of growth folds (Agri Valley near Alianello) in the prograding upper interval. In the Sarmento Synthem, in contrast, growth strata are absent. The dip directions of the growth strata show that in the retrograding lower interval of the Sinni Synthem the eastern margin of the Sant'Arcangelo synform tilted toward the SW (Fig. 23.11a), whilst in the prograding upper interval (poorly represented in Fig. 23.11a but well exposed north of the transect) the western margin of the synform tilted toward the NE.

The Sinni Synthem is unconformably overlain by braid-plain conglomerates (Castronuovo Conglomerate) interfingering with lacustrine deposits (San Lorenzo clay). The Castronuovo Conglomerate (unit 5a in Fig. 23.8) is well exposed along the western and northern margins of the Sant'Arcangelo synform. It consists of scour-based, clast-supported conglomerates showing common pebble imbrication, well-preserved large-scale foresets and evident trough-fill cross-stratification. The San Lorenzo clay (unit 5b in Fig. 23.8; part of the San Lorenzo cycle of Pieri *et al.*, 1994) is represented by lacustrine mudstones and subordinate siltstones containing several volcanoclastic layers (Caggianelli *et al.*, 1992). Marginal lacustrine deposits characterized by coarse-grained sharp-based debrites and sporadic thin layers of calcareous tufa were also recognized in the Serra Corneta area. West of Alianello, growth strata testifying westward tilting movements were observed in the lower part of the San Lorenzo lacustrine deposits. We do not know whether these features were produced by the growth of the Tursi–Rotondella thrust system or by folds in the allochthonous sheets related to the reactivation of the Apennine duplex system.

East of the Nocara ridge, the coarse-grained deposits of the Sinni Synthem and the overlying Castronuovo Conglomerate plus San Lorenzo clay are substituted by the upper portion (0.92–0.70 Ma, Fig. 23.6) of the Sub-Apenninic Clay and by the overlying (0.70–0.66 Ma) Montalbano Sandstone (Ciaranfi *et al.*, 1996a, b). This portion of the Sub-Apenninic Clay unit has been carefully investigated by Ciaranfi *et al.* (1996a,b) and Marino

(1996a,b) in the Montalbano Ionico composite section (interval IIA of these authors) where it includes the volcanoclastic layers V_2, V_3 and V_4. The upper portion of the Sub-Apenninic Clay is temporally confined within the NN19f nannofossil zone, with the Lower/Middle Pleistocene boundary just above the V_4 volcanoclastic layer. In the Montalbano section, the interval mostly consists of inner-shelf mudstones showing a deepening episode just above the V_4 horizon. It is possible that the maximum encroachment at the top of the retrograding lower interval of the Sinni Synthem correlates with this deepening event. The absence of coarse clastic deposits in this portion of the Sub-Apenninic Clay is justified by the morphological confinement created by the growing Nocara ridge, which prevented a direct coarse-grained supply from the Sinni–Synthem fan-delta systems.

Between the Agri and Cavone rivers the Sub-Apenninic Clay grades upward into the Montalbano Sandstone which consists of nearshore poorly-cemented sandstones including several volcanoclastic layers (interval IIB and V_5–V_9 volcanoclastic beds in Ciaranfi *et al.*, 1996a,b). The Sub-Apenninic Clay and Montalbano Sandstone couplet testifies to a coarsening-upward prograding shelf system, related to the forward migration of the active thrusts, in which the Montalbano shoal-water sandstones represent a sandy shelf bordering a braid-plain system represented by the coeval Castronuovo Conglomerate. Seismic profiles across the southern transect clearly depict the downdip facies architecture of the upper portion of the Sub-Apenninic Clay and show the continuous progradational characteristic of this depositional unit expressed by an offlapping succession of shelf, slope and base-of-slope deposits (Fig. 23.11b). On top of the allochthonous sheets an almost reflection-free unit, just showing some low-amplitude and low frequency discontinuous reflectors, seismically images the shelf portion of the Sub-Apenninic Clay. In correspondence to the nappe front, the shelf muddy deposits pass into an apron of offlapping slope mudstones, which laterally evolve into a prominent channel-fill complex developed at the foot of the slope. This lateral transition is clearly shown in seismic profiles by weak and discontinuous rugged reflectors with sigmoid to tangential/oblique configuration laterally replaced by a channel-in-channel complex array of strong reflectors with negative relief. The complex architecture of this slope system testifies to a delta-fed apron cut at the toe by a progressively filled axial channel system. Northeat of San Basilio 2, the channelized system is substituted by a package of weak reflectors displaying an overall aggrading to prograding mounded configuration (basin-floor mounded turbidite lobes). The mounded deposits laterally grade into a sheet-like stratal unit characterized by an overall thinning-upward stacking pattern of thin bedded sandy turbidites (well represented in Pomarico 4) seismically imaged by discontinuous subparallel to gently-downlapping reflectors (basin-floor turbidite sheet-lobes complex) (Fig. 23.11c). Toward the foreland, gravel-rich cross-stratified large sand waves separated by reactivation surfaces give evidence of active reworking by bottom currents with longitudinal dispersal. In the Matera–Gravina area, these terrigenous deposits lap by pinch out onto carbonate-ramp deposits (Gravina Calcarenite, Fig. 23.6 and unit 5e in Fig. 23.8). A thin veneer of glauconite-rich foraminiferal mudstones drapes the latter. These condensed deposits represent the downlap termination of the offlapping muddy slope the progressive northeastward migration of which created over time a foundation onto which the shelf prograded. Younger Pleistocene deposits cut across by the section, but having no seismic resolution in Figure 23.11 are represented by coarsening-upward shelf mudstones with *Gt. truncatulinoides excelsa, Hyalinea baltica* and *Gephyrocapsa parallela* (Gravina clays; Fig. 23.6) which overlie the condensed mudstones draping the Gravina Calcarenite. These open-shelf muddy deposits, lateral to the nearshore Montalbano Sandstone, represent the progressive infilling of the foredeep basin related to the progradation of the shelf over the previous starved basin as far as the outer margin of the Bradano trough. In this area, southwestward-tilted strong reflectors at the top of the Gravina Calcarenite indicate a persistent flexural subsidence of the foreland ramp up to the beginning of the Middle Pleistocene.

Younger Quaternary deposits cropping out in the southern-transect area, but not crossed by the

section of Figure 23.9, are represented by the Serra Corneta Conglomerate in the Sant'Arcangelo synform and by the Monte Marano Sandstone and Irsina Conglomerate in the Bradano trough (Fig. 23.6; units 3 and 4 in Fig. 23.8), as well as by Middle–Upper Pleistocene terraced shallow-marine deposits (unit 2 in Fig. 23.8). The Serra Corneta Conglomerate consists of even-parallel beds of red-stained, weathered alluvial conglomerates overlying a metre-thick horizon of reddish subaerial soil (Vezzani, 1967; Pieri *et al.*, 1994). It is probable that the palaeosol at the base of the Serra Corneta Conglomerate temporally corresponds to the Monte Marano sandstones, both marking a moment of tectonic quiescence when the Apulia flexural subsidence had stopped and the tectonic rebound of the mountain chain had not yet started. The beginning of this post-compression uplift coincided with the establishment of the Irsina prograding fluvio-deltaic system in the Bradano trough and with the sedimentation of the Serra Corneta Conglomerate on the outer slope of the mountain chain.

Intermediate cross section

This section, located some kilometres north of the southern transect, cuts across the frontal ramp of the allochthonous sheets and the western part of the foredeep basin (Figs 23.8, 23.12). In this area, the higher morphological relief created by repeated breaching of the thrust toe and the confinement of the foredeep basin determined by the faulted and tilted Apulia carbonates produced a sedimentary facies architecture quite different from that of the southern transect (Figs 23.11b, 23.12).

The 3.70–2.13 Ma interval discontinuously drapes the Apulia carbonates and is represented, as in the southern transect, by foraminiferal limestones containing *Gt. puncticulata* and *Gt. bononiensis* overlain by condensed hemipelagic marls with *Gt. crassaformis* (Fig. 23.12). These deposits are overlain by a thick pile of silicoclastic turbidites commonly yielding *Gb. inflata* (2.13–1.83 Ma interval). This turbidite system forms a clastic wedge of aggrading to prograding basin-floor sandstone lobes displaying evident onlapping terminations. Synsedimentary tectonics affecting the foreland ramp in this time interval is manifested by growth faults, as well as by tilted and truncated sandstone bed-sets. The *Gt. inflata* turbidites are seismically characterized by strong and fairly continuous parallel reflectors with moderate to high amplitude and frequency. Well-logs show well-defined cylinder-shaped SP curves in the western portions of the basin (Torrente Salandrella 1 from 1800 to 2675 m) and serrated bell-shaped profiles in the eastern ones (Pizzo Corvo 1 from 1679 to 1982 m).

The most prominent depositional feature of the foredeep basin is represented by a large synramp clastic wedge (1.83–1.50 Ma interval in Fig. 23.12) forming a prograding slope-fan system mostly made up of offlapping mud-flow deposits (weak seismic reflectors with chaotic configuration and linear shaly SP curves) and channelized sandy or pebbly turbidites (discontinuous weak reflectors associated with irregular, concave-upward strong reflectors; variable shapes of the well-log profiles depending on the grain-size of the infilling sediment and on the position inside the basin). The line drawing shows three major aggrading/prograding fans separated by large erosional channels, the lower one appearing as a large multi-storey and backstepping channel filled with longitudinally dispersed pebbly sandstones (Pizzo Corvo 1 between 1530 and 1625 m, mostly characterized by a serrated blocky log shape). The lower boundary of the wedge is marked, as in the previously described sections, by a very strong continuous reflector, locally appearing as a truncation surface, which corresponds to the widespread condensed section interpreted in the southern transect as the downlap termination of the Craco Clay unit.

The synramp wedge is overlain by a lens-shaped onlap-slope system (1.50–1.25 Ma interval in Fig. 23.12) made up of very thin-bedded turbidites, characterized in well logs by linear to rounded spiky SP profiles, which are cut downdip by channels filled with longitudinally dispersed pebbly sandstones and conglomerates (highly resistive conglomeratic beds in Pizzo Corvo 1 between 1030 and 1180 m). This retrogressive system appears basically to have been constructed by resedimented debris reworked from the previous, tectonically active, oversteepened slope, as testified by sets of chaotic reflectors indicating slope failures.

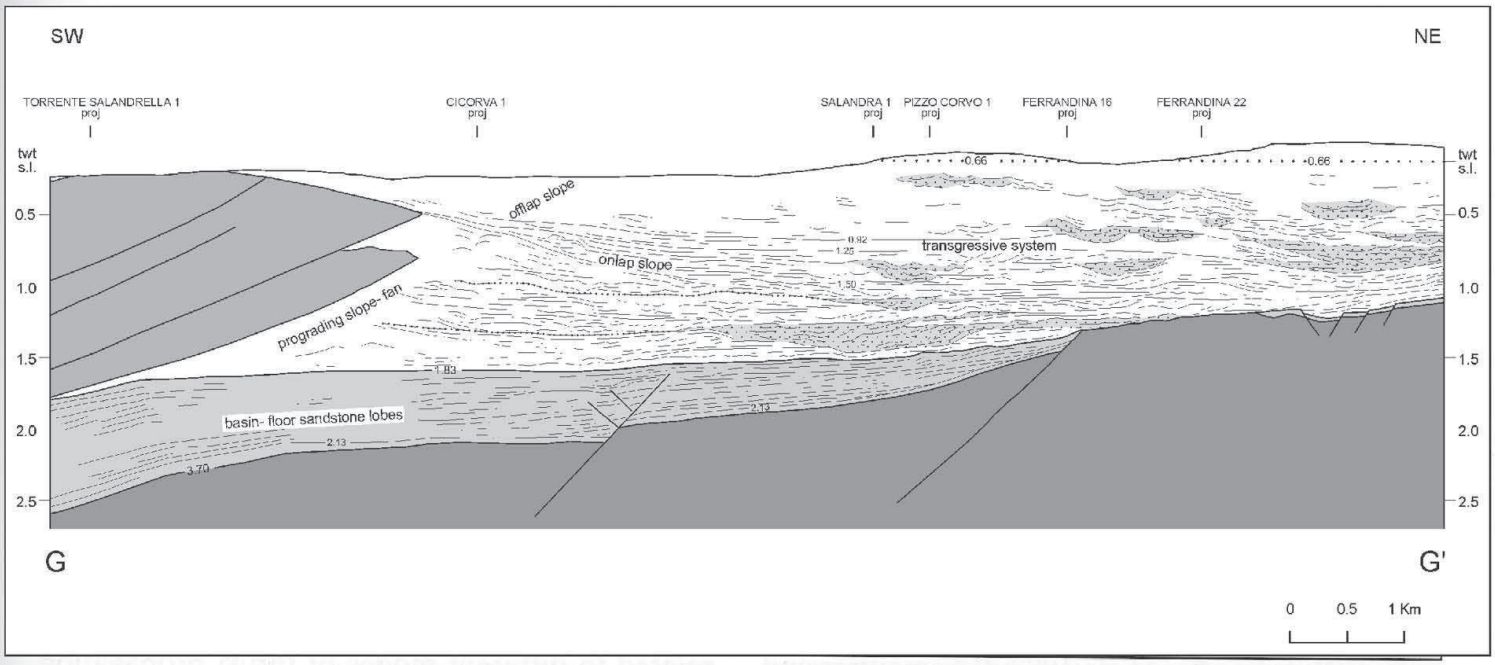

Figure 23.12 Line drawing across the Apenninic margin and the foredeep basin in the Salandra area (seismic line provided by AGIP; see location in Figure 23.8; vertical scale in seconds (TWTbelow sea level).

The 1.25–0.92 Ma interval of Figure 23.12 is represented, as in the southern transect, by a thin sheet of transgressive mudstones which basinward are overlain by coarse-grained deposits by means of an erosional surface. In the southern area, a wide shelf floored by the Apenninic nappes experienced a generalized marine flooding during this time interval (Figs 23.6, 23.9); in the whole northern area, in contrast, the marine transgression was limited to the frontal part of the allochthonous sheets because of the higher topographic relief created by the nappe imbrication.

The 1.25–0.92 Ma transgressive system is disconformably overlain by a thick clastic wedge (0.92–0.66 Ma interval in Fig. 23.12) forming the bulk of the Sub-Apenninic Clay unit in the area. Some volcanoclastic layers, possibly corresponding to the V_1–V_4 horizons of Figure 23.6 were recognized in the subsurface (Cicorva 1 and Salandra 1 wells). Figure 23.12 shows the inner portion of the wedge consisting of nearly reflection-free deposits with few weak reflectors suggesting an oblique progradational configuration. The slope deposits, characterized in well-logs by shale-prone spiky SP curves (low-density turbidite accumulation), pass basinward into a prominent system of erosional channels, seismically imaged by nested large-scale concave reflectors, which have been filled by well-defined stacks of fining- and thinning-upward sequences of sandstones and pebbly sandstones (Ferrandina 22 well). These channel-fill coarse-grained deposits were probably fed by the upper portion of the Serra del Cedro fan-delta conglomerates (unit 5a in Fig. 23.8) cropping out about 20 km NW of the section (Loiacono and Sabato, 1987).

The offlap-slope system is overlain, as in the southern transect, by shelf mudstones lacking any seismic response in the subsurface. This uppermost part of the Sub-Apenninic Clay unit is finally overlain (0.66 Ma dotted line in Fig. 23.12) by prograding barrier sandstones (Monte Marano Sandstone) and fluvio-deltaic coarse-grained deposits (Irsina Conglomerate, units 3 and 4 in Fig. 23.8).

BASIC RELATIONSHIPS BETWEEN THRUST PROPAGATION AND SEDIMENTATION

Relationships between active compressional tectonics and the sedimentary record in foredeep and satellite basins have been extensively investigated in order to better understand the kinematic evolution of mobile thrust-belt (Riba, 1976; Ori and Friend, 1984; Castellarin *et al.*, 1986a; Ori *et al.*, 1986, 1991, 1993; Ricci Lucchi, 1986a, b; Nichols, 1987; Vai, 1989; Beer *et al.*, 1990; Mutti, E., 1990, 1992; Van Mount *et al.*,

1990; Specht *et al.*, 1991; Puigdefabregas *et al.*, 1992; Suppe *et al.*, 1992; Zoetemeijer *et al.*, 1992, 1993; Deramond *et al.*, 1993; Mellere, 1993; Peper, 1993; Zoetemeijer, 1993; Burbank and Vergés, 1994; Hardy and Poblet, 1994; Millan *et al.*, 1994; Poblet and Hardy, 1995; Storti and McClay, 1995; Gimenez-Montsant and Salas, 1997; Hardy and Ford, 1997; Meigs and Burbank, 1997; Mugnier *et al.*, 1997; Poblet *et al.*, 1997; Schlunegger *et al.*, 1997; Sissingh, 1997; Storti and Poblet, 1997; Yellin-Dror *et al.*, 1997). Nevertheless, reliable predictive models of thrust-related depositional sequences are still lacking, particularly in duplex systems, owing to several difficulties in applying the conceptual models of sequence stratigraphy to a mobile thrust-belt–foredeep system (Posamentier *et al.*, 1988; Posamentier and Vail, 1988; Emery and Myers, 1996; Miall, 1997). Considering that in compressional systems the tectonic activity can largely overprint the effects of eustatic sea-level fluctuations (Zoetemeijer *et al.*, 1993), we have assumed, in the analysis of the Southern Apennines, that significant changes in the relative sea-level and, consequently, significant changes in the accommodation space were mostly produced by flexural subsidence in the foredeep basin and by flexural subsidence plus thrust activity in the mountain chain. This means that the progressive, although differential across adjacent segments, forward migration of the equilibrium points in the foreland "homocline" toward the Adriatic Sea was closely controlled by the lower-plate flexure-hinge retreat. The complex migration path of the equilibrium points across the outer margin of the mountain chain results instead from the interplay between flexural deflection (deepening of the sole thrust) and active-thrust trajectories (uplift related to the displacement of the hangingwall blocks). Maximum addition of space above the tectonic wedge and maximum landward migration of the equilibrium points took place during periods of out-of-sequence thrust propagation and duplex breaching, when the thrust toe was inactive and the new space added above the toe equalled the flexural deflection of the lower plate. Conversely, minimum migration of the equilibrium points on top of the thrust toe occurred when the nappes advanced over a gently dipping sole thrust (active long flat) and the vertical component of the forward displacement roughly equalled at every point the flexural subsidence. The Apennine thrust-sheet-top deposits and the adjacent foredeep sedimentary units reveal very different sedimentary responses to these end-members of the thrust propagation mode. These responses are represented by widespread high-energy marine fan-delta systems in the first case, the great volume of sediment supply being related to the high rate of thrust-related uplift of the drainage basin, and by widespread low-energy-shelf deposits unconformably draping the allochthonous sheets in the second case.

In the following pages we shall re-examine the Pliocene–Pleistocene thrust-sheet-top and foredeep deposits in terms of stratigraphic signatures related to different modes of thrust propagation. Many problems may arise when we try to subdivide the entire depositional record into relatively small, discrete tracts, each of them representing the characteristic sedimentary response to a specific state of the thrust-belt–foredeep-foreland system. These difficulties derive from the number and the complexity of the variables (such as trajectories of the active thrusts and slip rates, time–space migration of the active thrusts, physiography of the mountain chain, climate, rates of flexural subsidence and flexure-hinge retreat). However, if the stratigraphic resolution is in the order of hundreds or even tens of thousand years, an approach based on the integration of the structural-geology tools and the sequence-stratigraphy methods may help to overcome these problems.

Generalizing the large variety of situations recognized in the Southern Apennines, the late kinematic evolution of the thrust belt–foredeep system and the mutual relations between tectonics and sedimentation may be described by a simple leitmotif recurrent through Pliocene and Pleistocene times:

(1) Forward (hinterland-to-foreland) transport of the allochthonous sheets shown by the progressive displacement of the nappe front toward the Apulia foreland;

(2) Interruption of the nappe advance on the foreland because of breaching processes in the tectonic wedge. In this phase of the tectonic process, the kinematic evolution of the mountain chain was controlled initially by a backward (foreland-

to-hinterland) migration of the active thrusts and subsequently by a forward thrust migration. In this second stage, the deepening of the sole-thrust trajectory and the propagation of the active thrusts toward the foreland domains caused the addition of new horses to the buried duplex system.

Following this leitmotif, mountain building in the Southern Apennines proceeded according to a caterpillar-like advancing mode, every stage of forward nappe transport having been preceded and followed by a significant telescopic shortening of the structural edifice behind the nappe front. This caterpillar-like kinematic behaviour allows the identification of well-defined tectonic cycles, each cycle starting with the activation of a long flat which played the role of a conveyor belt for the forward nappe transport and ending with the incorporation in the thrust belt of new segments detached from the lower plate. A tectonic cycle includes four major steps, each step following one another according to a fixed order, with some variations on the theme:

(1) Forward nappe transport over a long thrust flat (Fig. 23.13a);

(2) Breaching of the thrust toe near the tip line of the allochthonous sheets and development of a more or less steep frontal ramp (Fig. 23.13 b);

(3) Deactivation of the frontal ramp and backward migration of the active thrusts because of out-of-sequence thrust propagation (Fig. 23.13 c);

(4) Forward migration of the active-thrusts. In some cases forward thrust propagation caused the reactivation of the previously abandoned leading edge of the duplex system and the breaching of the thrust toe (Fig. 23.13d); in other cases the deepening of the sole thrust and the propagation of the active thrusts beneath and beyond the inactive leading edge caused the incorporation of new horses in the duplex system (Fig. 23.13e).

Other kinematic mechanisms active in the Southern Apennines during Miocene times, responsible for repeated changes from a duplex configuration to an imbricate-fan one and vice versa (Patacca *et al.*, 1992a), have not been dealt with in this chapter.

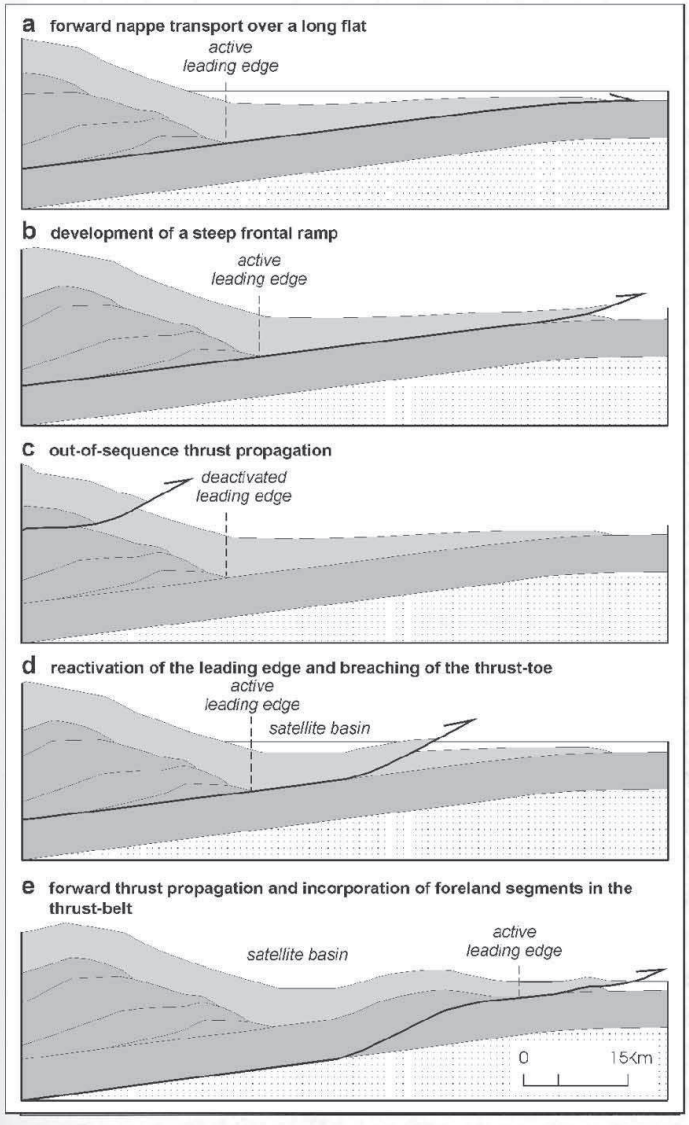

Figure 23.13 Diagrams showing various types of active-thrust trajectories (half arrows) controlling the sedimentation on top of the thrust sheets and in the foredeep basin.

FORWARD NAPPE TRANSPORT OVER A LONG THRUST FLAT

In the Southern Apennines, the clearest sedimentary response to a forward displacement of the tectonic wedge over a long thrust flat (Fig. 23.13a) is represented by the shallowing-upward Craco Clay–Sant'Arcangelo Sandstone couplet. These deposits unconformably drape older thrust-sheet-top deposits, as well as the Apennine allochthonous sheets.

Evidence for nappe advancing over a long thrust flat mostly derives from the following subsurface information:

(1) In the southern part of the study region, the allochthonous sheets tectonically cover without remarkable footwall cut-off thick upper Pliocene foredeep silicoclastic deposits (*Gt. inflata*-bearing

sandy turbidites), which in turn stratigraphically overlie condensed hemipelagic limestones containing *Gt. puncticulata*. Seismic sections tied by the Recoleta 1 well (located at a distance of 7–8 km from the nappe front) allow the identification of the *Gt. inflata* turbidites in the footwall of the Apenninic nappes as far as 12–15 km behind the present day nappe front. These geometric relations establish the minimum displacement of the Apenninic nappes after the deposition of the *Gt. inflata* turbidites;

(2) In correspondence to the Nocara ridge, that is 18–20 km SW of the nappe front, no sedimentary record of the *Gt. inflata* turbidites was found. In this area the Apenninic nappes tectonically overlie a wedge some hundred metres thick of *Gt. puncticulata*-bearing turbidites disconformably covering the Apulia carbonates (Tursi 1 Castelgrande, Rotondella 1, 2, 4 and Montegiordano 1 AGIP wells). This clastic wedge extends in the subsurface toward the mountain chain at least as far as the Tempa Rossa structure (D'Andrea *et al.*, 1993). These data demonstrate that just before the deposition of the *Gt. inflata* turbidites the allochthonous sheets had already reached the location of the future Tursi–Rotondella and Tempa Rossa tectonic structures. Consequently, they fix the maximum amount of displacement of the Apenninic nappes after the deposition of the *Gt. inflata* turbidites;

(3) At the end of the transport of the allochthonous sheets from the Tursi–Rotondella area to the present nappe front, the leading edge of the Apennine duplex system reached a final position close to that shown in Figure 23.2. This implies a length of the thrust toe of 30–40 km. Considering that the thickness of the allochthonous sheets did not exceed 4–5 km, this length requires a cohesive strength at the base of the nappes (Hsü, 1969) considerably lower than 200 bars and a pressure-overburden ratio of about 1.

As regards the timing, the nappe transport from the Tursi–Rotondella area to the present day position necessarily took place between 1.83 and 1.50 Ma, that is after the deposition of the upper Pliocene *Gb. inflata* turbidites and before the deposition of the Emilian thrust-sheet-top deposits which suture the nappe front (Fig. 23.11b). The occurrence of the Craco Clay and Sant'Arcangelo Sandstone on top of the allochthonous sheets provides additional constraints to the duration of the nappe transport. In theory, the Craco Clay–Sant'Arcangelo Sandstone couplet could have been deposited before, after or during the nappe transport. In reality, we can discard the first and the second possibilities because they would lead to the paradox that a displacement of 12–15 km would have occurred in a few tens of kiloyears, that is in the time interval representing the maximum range of uncertainty in our biostratigraphic constraints. These uncertainties concern the upper boundary of the *Gt. inflata* turbidites and the lower boundary of the Craco Clay in the first case (nappe transport before deposition of the 1.83–1.50 Ma interval), and the upper boundary of the Sant'Arcangelo Sandstone and the lower boundary of the Tursi Sandstone in the second case (nappe transport after the deposition of the 1.83–1.50 Ma interval). Conversely, if we admit that the transport took place during deposition of the Craco Clay–Sant'Arcangelo Sandstone couplet (Δt = 330 kiloyears) we obtain slip rates of 36–45 mm/a, which are realistic for areas characterized by high-rate flexure-hinge retreat accompanied by back-arc spreading (Argnani and Ricci Lucchi, this vol., Ch. 19).

The 3.70–3.30 Ma Pliocene deposits of the northern transect, displaying depositional features similar to those of the Craco Clay–Sant'Arcangelo Sandstone couplet, represent another example of a thrust-sheet-top unit deposited during nappe displacement over a long flat. Unfortunately, no constraints to fix the length of the thrust toe and the amount of displacement during this time interval are available in the northern part of the study area. Nevertheless, some useful information on the minimum displacement is still provided by the southern area. We have seen that before the deposition of the *Gt. inflata* turbidites, when the nappe front had already reached the Tempa Rossa and Tursi–Rotondella areas, the allochthonous sheets overlay the *Gt. puncticulata* turbidites. These deposits extended southwestward beneath the Apenninic nappes at least as far as the Outer thrust system, that is, to a distance of about 30 km from the present day nappe front. Therefore, the front of the allochthonous sheets had to move toward the foreland at least 15–18 km in about

400 ka (3.70–3.30 Ma). The resulting slip rates (37–45 mm/a) fit very well with those calculated for the Lower Pleistocene nappe displacement during deposition of the Craco Clay and Sant'Arcangelo Sandstone.

In conclusion, the sedimentary record on top of the thrust toe, when it moved toward the foreland domains above a long thrust flat, is represented in the Southern Apennines by a sheet of shallowing-upward deposits accumulated on a wide low-energy shelf adjacent to a low-gradient coastal plain. The shallowing-upward facies architecture reflects a progressive slight sea-floor uplift related to the vertical component of the forward nappe transport over a gently dipping (6°–7°) sole-thrust surface not compensated for by the synchronous flexural subsidence. In the foredeep basin, condensed mudstones interpreted as the downlap termination of the shelf thrust-sheet-top deposits represent the basinward equivalent of the nappe sheet drape. This condensed section, seismically imaged by a continuous strong reflector, corresponds to the major unconformity surface, which establishes the sequence boundary.

DEVELOPMENT OF A STEEP FRONTAL RAMP AT THE EDGE OF THE NAPPE SYSTEM

The front of the Southern Apennine thrust system is everywhere represented by a prominent frontal ramp developed after the previous stage when a remarkable displacement of the allochthonous sheets over a long thrust flat had occurred. The sedimentary response to the ramp growth is recorded in the foredeep basin by an impressive and abrupt change of facies. On top of the thrust-sheets, in contrast, the sedimentary response is not evident, due to the persistent low-energy-shelf sedimentation during the time interval in which the frontal ramp was active.

Clear examples of synramp thrust-sheet-top deposits were recognized only in seismic profiles of the southern transect. Here wedge-shaped aggradational packages of reflectors showing intraformational unconformities closely controlled by the growth of the frontal imbricates feature small satellite basins at the rear of the active nappe front.

In the foredeep basin, the development of a steep frontal ramp in correspondence to the edge of the nappe system (Fig. 23.13b) is recorded by the accumulation of a thick wedge of prograding slope-fan deposits in the subsiding footwall block, progressively upward truncated by the rising hangingwall (Figs 23.10b, 23.11b, 23.12). The different amounts of the hangingwall displacement in Figures 23.10b, 23.11b and 23.12 suggest different time duration of the active frontal ramps. The duration did not exceed 25–50 ka in the southern and northern transects where the displacement ranges between 1 and 2 km (average slip rate: 40 mm/a), but it was probably slightly longer in the intermediate section where the displacement is greater than 3.5 km. The slope-fan wedge in the footwall of the frontal ramp is basically constituted by gravity-driven deposits largely derived from the "cannibalization" of unconsolidated thrust-sheet-top deposits overlying the frontal part of the allochthonous sheets. The overall geometry, the internal facies distribution and the sand-body architecture of the slope-fan system were primarily controlled by the nature of the drainage-feeder system and by the volume and grain-size of the sediment supply. Differences in sediment properties moving parallel to the nappe front are principally related to the topographic relief of the thrust toe inherited from the cumulative array of the previous thrusts. Minor variations influencing sediment transport and redistribution in the basin are related to the local configuration of the foreland "homocline" which determined more or less confined basin architectures. Figures 23.10b, 23.12 and 23.11b are representative of two end-member types of thrust-related slope-fan systems, one related to the high relief and the other to the low relief of the thrust toe. Both types of system display a predictable arrangement of the main architectural elements, including the overall facies distribution and the geometry of the sand bodies. Figures 23.12 and 23.10b, representative of the northern segment of the Lucania Apenninic margin, give a good example of a highly-confined aggrading to prograding channelized slope-fan system with a gravel-rich slope apron basically accreted by

reworking and submarine catastrophic mass-wasting of the tectonically active steep margin. The depositional products reflect a wide variety of gravity-flow processes, including: (1) slumps of fine-grained deposits locally embodying exotic blocks in the steep upper slope incised by numerous low-relief channels, (2) widespread channelized sandstones and conglomerates in the mid-slope and toward the edge of the system, (3) turbidite lobe deposits coalescing into fringing sand-sheets and directly onlapping against the outer margin of the basin. Coarse-grained clastic wedges are typically fed by fan-delta systems directly accumulated onto a high-declivity subaqueous slope. The existence of a slope-type fan-delta system in the area is testified in the subsurface (Loiacono and Sabato, 1987) by a thick pile of conglomerates and pebbly sandstones accumulated in the footwall of the active frontal ramp (Basento 1 between 720 and 1480 m). Figure 23.11b shows the typical configuration of the thrust-related slope-fan system in the southern segment of the Lucania Apenninic margin where the flat morphology of the thrust toe allowed the establishment of a wide shallow shelf on top of the allochthonous sheets during the development of the frontal ramp. In this case a relatively unconfined and moderate-efficiency system set up, mainly characterized by prograding depositional lobes. Three basic architectural elements, having clear laterally-interbedded relations, are recognizable: an inner channel-levee system, a stack of mounded lobes attached to the ends of the leveed channels and over which the muddy levees spread out, and finally a broadly parallel-layered turbidite unit which onlaps against the outer margin of the foredeep basin.

DEACTIVATION OF THE FRONTAL RAMP AND BACKWARD MIGRATION OF THE ACTIVE THRUSTS BY OUT-OF-SEQUENCE THRUST PROPAGATION

The deactivation of the frontal ramp caused by the backward migration of the active thrusts has an unequivocal stratigraphic signature in the foredeep basin (Fig. 23.13c). On top of the allochthonous sheets, in contrast, the sedimentary response to this important change in the active-thrust trajectories closely depended on the physiography of the thrust toe.

The southern transect provides a very good Pleistocene example of the relation between tectonics and sedimentation during backward thrust propagation when not only in the foredeep basin, but also above the deactivated thrust toe, any addition of accommodation space was entirely determined by the flexural subsidence. On top of the allochthonous sheets, the deactivation of the frontal ramp (early stage of the backward thrust migration) is manifested by the establishment of a shoal-water retrograding fan-delta system facing a widespread shelf area (lower part of the Sarmento Synthem laterally grading into the Tursi Sandstone, Fig. 23.9; note that at this time the Nocara ridge had not yet formed). Maximum out-of-sequence thrust propagation (late stage of the backward thrust migration) and consequent maximum accommodation space above the Apenninic nappes occurred between 1.25 and 0.92 Ma when the maximum landward migration of the marine facies took place (unit 3 in Fig. 23.9). In the foredeep basin, the persisting flexural subsidence coupled with the diminished sediment supply related to the retreat of the source area allowed the establishment of an onlap-slope system followed by a transgressive one, with deeper-water deposits progressively onlapping the inner (southwestern) flank of the basin made by the edge of the inactive thrust toe. The sediment supply basically derived from the erosion of the shelf-edge/slope and from longitudinally driven currents related to submarine valley systems. Above the onlap-slope front a gentle depositional slope became established during the late stage of the backward thrust propagation.

The deactivation of the frontal ramp took place at about the same time in both the northern and southern segments of the Lucanian Apenninic margin. Nevertheless, due to the higher topographic relief of the nappe front and to the oversteep profile of the synramp wedge, a widespread destructional slope system developed in the northern segment during the 1.50-1.25 Ma interval (Figs 23.10b, 23.12), with an onlapping base-of-slope apron basically supplied by extensive mass-wasting of materials from the shelf-edge and upper-slope areas.

The 3.30–2.50 Ma Pliocene thrust-sheet-deposits described in the northern and southern

transects (Figs 23.5, 23.6) represent another noticeable example of clastic sedimentation on a passive shelf floored by an inactive thrust toe, open toward the foredeep basin and limited hindward by backstepping out-of-sequence thrusts.

In conclusion, the deactivation of the nappe frontal ramp is recorded on top of the allochthonous sheets by a deepening-upward fan-delta/ shelf system with maximum marine flooding in correspondence to the maximum out-of-sequence thrust propagation. In the foredeep basin this change of kinematic behaviour is recorded by a low-energy onlap-slope system suturing the front of the allochthonous sheets and overlain by a transgressive system that marks the moment of maximum out-of-sequence thrust propagation.

FORWARD MIGRATION OF THE ACTIVE THRUSTS

Our reconstruction of the upper Pliocene–Middle Pleistocene kinematic evolution of the Southern Apennines shows that stages of out-of-sequence thrust propagation have systematically been followed by stages of forward thrust migration. Forward thrust migration proceeded according to three kinematic processes: re-approach of the active thrusts to the previously abandoned leading edge of the duplex system without important remobilization of the latter; reactivation of the leading edge and breaching of the thrust toe (Fig. 23.13d); deepening of the sole thrust, active thrust propagation beneath and beyond the abandoned leading edge and incorporation of new horses into the duplex system (Fig. 23.13e). These processes did not necessarily follow one another; in the southern transect, in fact, thrust propagation beyond the abandoned leading edge followed maximum out-of-sequence thrust propagation without breaching of the thrust toe.

A case of out-of-sequence thrusts re-approaching the previously abandoned leading edge of the duplex system without remobilization of the latter is illustrated by the 2.50–1.83 Ma upper Pliocene interval in the southern transect (Fig. 23.6). In correspondence to the surface projection of the inactive leading edge, prograding sand-rich fan-delta-front deposits stratigraphically overlying lagoon–prodelta mudstones represent this interval. These deposits grade eastward into shelf sandstones and mudstones. The stratal geometry and the facies distribution depicts a wide shelf unaffected by synsedimentary deformation, where the progradational characteristic of the fan-delta-front deposits can be related to an increase in volume and calibre of the sediment supply caused by the rejuvenation of the drainage basin controlled by the tectonic uplift in the mountain chain. It is interesting to note that the internal architecture of depositional systems related to the re-approach of out-of-sequence thrusts to the previously abandoned leading edge of a duplex system is the mirror image of that produced by the out-of-sequence thrust propagation. Referring to an imaginary receiver located on top of the thrust toe in front of the surface projection of the duplex leading edge, the difference is only represented by the migration trend of the tectonic activity. Active thrusts moved toward the far-field during out-of-sequence thrust propagation (overall retrogradational geometry with maximum accommodation space above the thrust toe, maximum backstepping of the deltaic systems on top of the allochthonous sheets and maximum landward migration of the marine facies in the late stage of the backward thrust migration) and toward the near-field during forward thrust propagation when out-of-sequence thrusts re-approached the previously abandoned leading edge (overall progradational geometry, the sediment supply exceeding the accommodation volume). In conclusion, far-field and subsequent near-field migration of the active thrusts can be reflected, on top of the allochthonous sheets, by complete transgressive-regressive cycles without any internal discontinuity if the leading edge of the duplex system did not undergo reactivation.

The case of reactivation of the leading edge and breaching of the thrust toe is schematized in Figure 23.13d. In this case a satellite basin is established on top of the nappes in the hangingwall of the breach. Obviously, the internal geometry of the duplex system, including the shape of the sole thrust, may have been in real cases quite different from this schematization. For example, the long thrust flat separating the transported Apulia carbonates from the autochthonous ones might

have been substituted by a hinterland-directed, deepening staircase trajectory. A good example of sedimentary response to the reactivation of a previously abandoned leading edge with consequent breaching of the thrust toe is represented by the upper Pliocene fan-delta deposits filling the Ofanto basin in the northern transect (fan-delta deposits post-dating 2.50 Ma in Fig. 23.10a). Figure 23.10a shows the complex stratal geometry of the fan-delta deposits filling the satellite basin. This stratal configuration results both from the growth of the ramp anticline in the hangingwall of the breach (progressive tilting toward the SW in correspondence to the accommodation fault) and from the uplift of the growing San Fele antiformal stack (synsedimentary tilting toward the NE of the upper part of the growth strata). Note that the horses of Apulia carbonates, which are supposed to underlie the San Fele antiformal stack, had in any case not yet formed when the Ofanto satellite basin began to develop (unit 8 in Figure 23.9).

Breach processes similar to those which produced the Ofanto satellite basin theoretically could have developed during a backward thrust migration, according to a thrust geometry identical to that shown in Figure 23.13d. Nevertheless, such features have never been recognized in the Southern Apennines.

A different mode of forward thrust migration is given by the deepening of the sole thrust and the generation of a new thrust flat beneath and beyond the inactive leading edge (Fig. 23.13e). In such a way, younger and more external horses have been added to the tectonic wedge beneath the roof thrust. In this stage, satellite basins develop on top of the allochthonous sheets between the surface projection of the inactive leading edge and the growing new ridge. This type of satellite basin and the previous one (Ofanto basin) has similar stratigraphic signatures in spite of the fact that they formed in different structural settings, at the rear of a new leading edge and ahead of a reactivated pre-existing leading edge respectively.

The Sinni Synthem offers a very good example of a satellite basin developing at the rear of a new leading edge, generated by the forward propagation of the active thrusts in the Apulia carbonates from the foot of the Apenninic duplex to the front of the Tursi–Rotondella thrust system. Figure 23.11a shows only the lower part of the satellite-basin fill deposits. The upper one, represented by the uppermost portion of the Sinni Synthem overlain by the Castronuovo Conglomerate and the San Lorenzo clay, is well exposed northwest of the section. The diachronous unconformity at the base of the Sinni Synthem and the progressive backward (westward) tilt of the eastern margin of the basin indicated by growth strata in the lower interval of the Sinni Synthem establish that the uplift of the Nocara ridge on top of the growing Tursi–Rotondella thrust system began around 0.92 Ma and not around the Pliocene–Pleistocene boundary as is usually reported in the geological literature (Hippolyte *et al.*, 1994b). Note that in the case of the Nocara ridge the emergence of the active thrust responsible for the growth of the ramp anticline had quite a different trajectory from that shown in Figure 23.13e. This is because the displacement in the Apulia carbonates was compensated in the roof units partly by fault-propagation folds and partly by back-thrusts cutting across the allochthonous sheets. The latter are particularly well developed in correspondence to a shallow triangle zone at the northern termination of the structural high. In our opinion the thrust propagation from the foot of the Apenninic duplex system to the Outer thrust system in the north and to the Tursi–Rotondella thrust system in the south did not proceed simultaneously (Fig. 23.2). We believe that the active leading edge responsible for the Stigliano breach was still located at the foot of the Apennine duplex system while the sole thrust had already reached the Tursi–Rotondella area south of the Scorciabuoi fault. In a second stage, forward thrust propagation occurred also in the northern segment and the Outer thrust system developed ahead of the deactivated front of the Apenninic duplex. This implies that the bulk of the shortening across the Tursi–Rotondella thrust system results from the sum of the shortening across the Stigliano breach and the shortening across the Tempa Rossa upthrust structure. Balanced cross-sections suggest about 6 km of horizontal displacement in the Tursi–Rotondella structure versus a maximum of 3 km in the Tempa Rossa one.

It is noteworthy that forward thrust propagation in the Lucania Apennines was followed by (and perhaps coexisted with) episodic reactivation of the previously abandoned leading edge. This fact is well documented by the internal stratal geometry of the upper interval of the Sinni Synthem characterized by growth strata showing a progressive forward (eastward) tilt of the western margin of the basin clearly related to a reactivation of the foot of the Apenninic duplex system. This reactivation is also confirmed by growth folds developed in the upper interval of the Sinni Synthem in the northern part of the satellite basin (small but spectacular anticline in the Agri Valley WSW of Alianello), formed as decollement folds or as fault-propagation folds at the termination of blind thrusts.

In the foredeep basin, the high rate of sediment supply coincident with a renewed deltaic progradation on top of the allochthonous sheets allowed the establishment of a well-developed prograding slope with a rapidly basinward-migrating offlap break and a rapid basin infilling with active fan sedimentation. The foredeep basin received large volumes of clastic material via turbidity currents and mass-flow transport processes because of the narrowing of the shelf produced by the forward migration of the active thrusts. Subaqueous sediment dispersal and consequent depositional geometry, though complex in detail, basically reflect the nature of the sediment feeder system. Large fan-delta-fed erosional channels filled with conglomerates characterize basins bordered by high-relief and steep-profile areas. Turbidite lobes and sheets, in contrast, characterize basinal areas facing low-relief feeder systems. The areal extension of the basin-floor turbidite lobes appears to have been strictly controlled by the geometry of the foreland "homocline".

SUMMARY AND CONCLUSIONS

Upper Pliocene and Pleistocene deposits unconformably overlying the roof units of the Apennine duplex system and disconformably covering the autochthonous Apulia carbonates in the Bradano foredeep basin display remarkable stratigraphic signatures which have been closely controlled by the thrust activity. Deformation in the study area did not proceed cylindrically, so that in the same time interval adjacent segments of the thrust belt may have undergone different kinematic evolution depending on the trajectories of the active thrusts. This fact prompts us to be very cautious when trying to perform correlations among widely spaced sections crossing the Apenninic chain. Nevertheless, characteristic stratigraphic signatures of the thrust-sheet-top and foredeep deposits related to well-defined trajectories of active thrusts represent helpful tools for reconstructing the time-space thrust migration. Thrust propagation followed in the Southern Apennines quite a simple leitmotif recurrent through late Pliocene and Early–Middle Pleistocene times. This dominant recurring theme describes mountain building similar to the advancing mode of a caterpillar, every stage of forward nappe displacement having been preceded and followed by a telescopic shortening of the structural edifice behind the front of the tectonic wedge. Considering the whole mountain chain and not only its frontal part, we see that during late Pliocene and Early–Middle Pleistocene times shortening took place as a continuous process and not as an alternation of periods of generalized tectonic activity with periods of tectonic quiescence, as has often been reported in the geological literature (such as in Patacca and Scandone, 1989). The old concept of "tectonic phase" takes into consideration only recurrent periods of forward nappe displacement and forward shift of the foredeep basin. In reality, in the late Pliocene-Pleistocene kinematic evolution of the Southern Apennines periods of forward nappe transport cover a limited fraction of the time in which shortening driven by passive lithospheric sinking acted as a continuous process (in our case 0.73 Ma versus 3.04 Ma). This implies that if we assume an average rate of horizontal displacement of 40 mm/a along the sole-thrust, the observed 30 km of cumulative forward nappe displacement between 3.70 and 3.30 Ma and between 1.83 and 1.50 Ma have a counterpart of about 90 km of cumulative internal shortening of the tectonic wedge between 3.30 and 1.83 Ma and between 1.50 and 0.66 Ma. An accurate computation of the total shortening and shortening partition based on balanced cross-sections is beyond the aims of this study. Here we just wish to

stress the fact that very important processes contributing to the construction of the mountain chain took place during periods in which the outer margin of the thrust belt was not affected by any tectonic activity except flexural subsidence. In terms of major structural features, significant products of internal shortening in the absence of thrust activity along the outer margin of the mountain chain are represented by the following:

(1) Considerable thickening of the tectonic wedge. The sole thrust of the Southern Apennine mountain chain lies at depths exceeding 20 km in correspondence to the Tyrrhenian coast (seismic line CROP-04, Mazzotti *et al.*, 2000);

(2) Important modifications of the original lower Pliocene Apulia-carbonate duplex system which include both out-of-sequence re-imbrication and in-sequence addition of new horses; repeated breaching and imbrication of the thrust toe; development of new duplex systems within the rootless Apenninic nappes. These shallow duplex systems form, in some cases, huge antiformal stacks more than 5000 m thick.

The reconstruction of the late Pliocene and Early–Middle Pleistocene kinematic evolution of the Southern Apennines has allowed the recognition of tectonic cycles, each cycle starting with the activation of a long thrust flat playing the role of conveyor belt for nappe transport and ending with the deepening of the sole thrust and the propagation of active thrusts beneath and beyond the previous leading edge, with consequent incorporation of new horses into the duplex system. Tectonic cycles have been recorded in the foredeep basin and on top of the allochthonous sheets by thrust-related depositional sequences separated by major unconformities ($P_{1\text{-}2}$ and $Q_{1\text{-}2}$ depositional sequences in Figs 23.5, 23.6). Figure 23.14 gives a synoptic representation of the stratigraphic signatures, on top of the roof units and in the foredeep basin, related to the different modes of thrust propagation in the Apennine duplex system. The figure mostly refers to the southern transect where the low topographic relief of the thrust toe allowed a more complete sedimentary record. Both $P_{1\text{-}2}$ and $Q_{1\text{-}2}$ depositional sequences have been divided into four systems tracts, each tract being representative of a well-defined step of the caterpillar-like motion of the tectonic wedge:

(1) *Active-thrust-flat systems tract*. On top of the allochthonous sheets this systems tract is represented by a drape of shallowing-upward, low-energy-shelf deposits (*nappe sheet drape*) overlying with angular unconformity the advancing nappes. In the foredeep basin this systems tract is represented by a *condensed section*, interpreted as the downdip termination by downlap of the previous thrust-sheet-top shelf deposits. The base of this condensed section coincides with a major truncation surface tracing in the basin the sequence boundary.

(2) *Active-frontal-ramp systems tract*. On top of the nappes this systems tract, usually indistinguishable from the upper portion of the underlying active-thrust-flat systems tract, is still represented by shallowing-upward low-energy-shelf deposits (*nappe sheet drape*). Locally it is represented by small clastic wedges deposited in minor satellite basins at the rear of the active frontal ramp. In the foredeep basin, the active-frontal-ramp systems tract is everywhere recorded by a rapidly prograding and relatively confined slope-fan system (*synramp wedge*) constituted by a thick wedge of gravity-driven deposits largely derived from the "cannibalization" of unconsolidated thrust-sheet-top deposits overlying the mobile frontal part of the allochthonous sheets.

(3) *Backward-thrust-migration systems tract*. It is represented on top of an inactive thrust toe by a deepening-upward, backstepping fan-delta system. The progressive landward migration of the equilibrium points related to the backward thrust migration was responsible for the retrogradational characteristic of the depositional sequence (*retrograding fan-delta/shelf system*), with maximum marine flooding (*transgressive system*) in the uppermost part of the tract during the late stage of the backward thrust migration, that is, when maximum out-of-sequence propagation of the active thrusts took place. In the foredeep basin, the backward-thrust-migration systems tract is characterized by a retrograding margin featured by an *onlap-slope system* and a *transgressive system* both dominated by incised to leveed channel fills, basinward grading into minor mounded turbidite lobes and sheet turbidites. The onlap-slope system

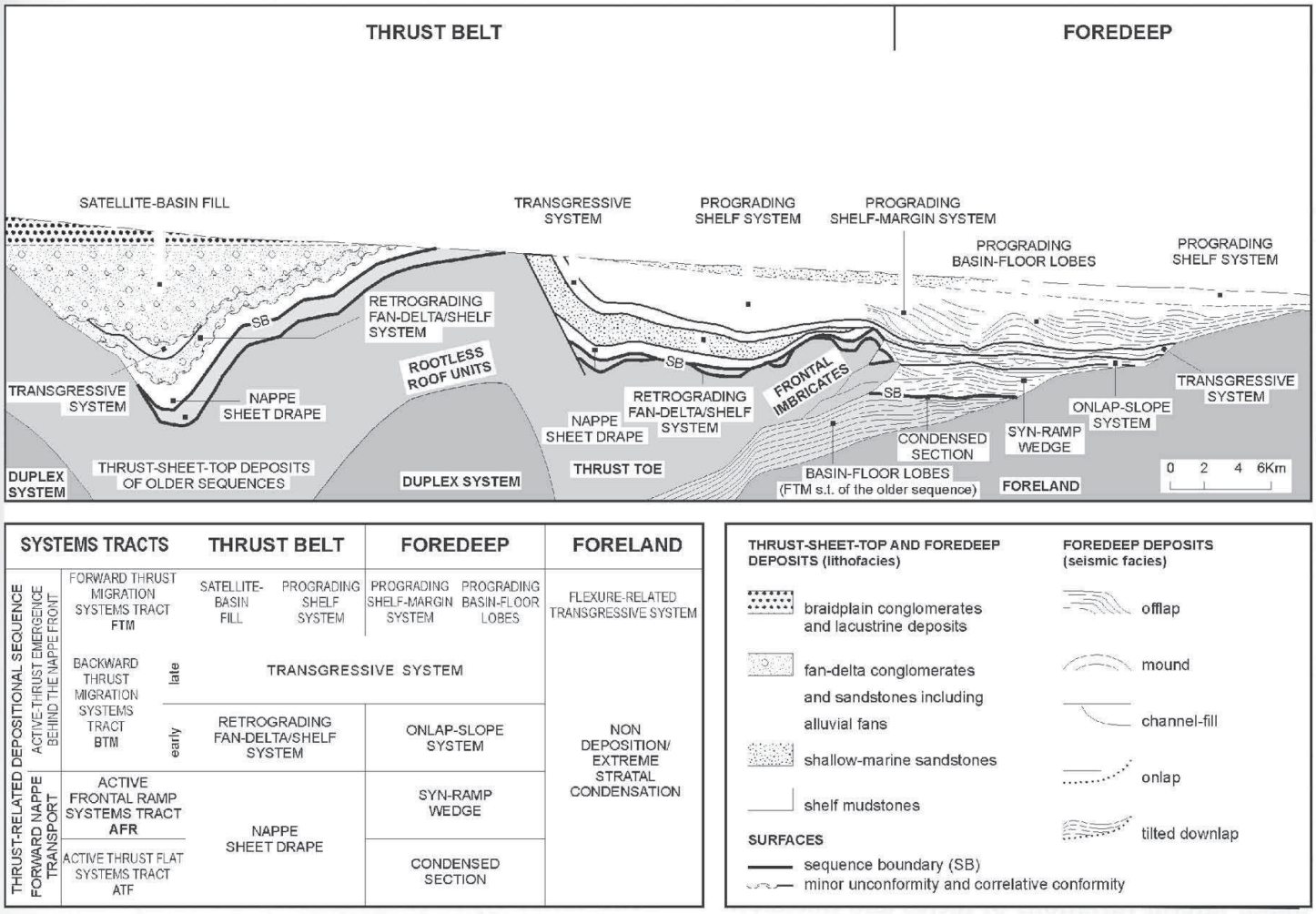

Figure 23.14 Thrust-related sequence stratigraphic model.

and the transgressive system indicate the deactivation of the frontal ramp (early stage) and the maximum marine flooding (late stage) respectively.

(4) *Forward-thrust-migration systems tract*. On top of the allochthonous sheets this systems tract is everywhere characterized by a fan-delta system having a progradational characteristic. The facies distribution and the internal stratal architecture of these deposits allow identification of two different depositional settings closely controlled by the active-thrust trajectories:

(a) Wide stable shelves with well-developed shoal-water fan-delta systems (*prograding fan-delta/shelf system*) when active out-of-sequence thrusts re-approached the previously abandoned leading edge without remobilization of the latter.

(b) Mobile satellite basins filled with very coarse-grained sedimentary units, characterized by diachronous basal unconformities and by growth strata featuring progressive angular unconformities at the basin margin (*satellite-basin fill*). Satellite basins developed either because of a breaching of the thrust toe ahead of the reactivated leading edge (Fig. 23.13d) or because of a forward thrust propagation in the Apulia carbonates which produced new horses in front of the abandoned leading edge (Fig. 23.13e). In both cases prograding systems (*prograding shelf system*) developed on top of the allochthonous sheets. In the foredeep basin, the forward-thrust-migration systems tract is represented by a rapidly prograding shelf-slope wedge (*prograding shelf-margin system*) and by widespread basin-floor turbidites (*prograding basin-floor lobes*).

In conclusion, the caterpillar-like motion of the Southern Apennine tectonic wedge has been recorded, step-by-step, by characteristic stratigraphic signatures both in the foredeep basin and on top of the allochthonous sheets. In the foredeep basin, major periods of sediment starvation correspond to moments of horizontal nappe

displacement and to moments of maximum out-of-sequence thrust propagation. Conversely, conditions of maximum terrigenous supply took place in two different tectonic settings:

(1) In the footwall of the frontal ramp, when a wedge of gravity-driven deposits (including mudflows, slides and olistostromes) laid down from the uprising hangingwall accumulated in a relatively confined basin;

(2) In front of a passive shelf, when forward thrust propagation caused rejuvenation of the feeder system and narrowing of the shelf domains, and a shelf-margin prograded over a relatively unconfined basin.

Conditions of low to moderate sediment supply correspond to moments of backward thrust propagation when an onlap-slope system was established on the retrograding foredeep margin.

In the thrust belt, three types of Pliocene to Middle Pleistocene thrust-sheet-top deposits can be distinguished:

(1) Shallowing-upward shelf mudstones fed by a mature drainage system, unconformably draping the forward-moving allochthonous sheets without major lateral variations of facies and thickness.

(2) Fan-delta and shelf marine deposits, floored by an inactive thrust toe, organized into fining-upward sequences during periods of backward thrust migration and into coarsening-upward sequences during periods of forward thrust migration in the absence of significant reactivation of the previously abandoned leading edge. The overall geometry and facies architecture of these depositional systems strictly depends on the rate and amount of the drainage-basin uplift and on the width of the shelf determined by the shortening of the thrust toe caused by the cumulative thrust displacement;

(3) Predominant coarse-grained deposits of alluvial/fan-delta, and minor shelf deposits characterized by synsedimentary deformation, accumulated in satellite basins on top of the roof units. Three types of satellite basins have been distinguished, based on the tectonic setting. The first type of basin, recognized in seismic profiles but not yet identified on the surface, is represented by small clastic wedges with evident growth strata developed at the rear of the active frontal ramp of the Apenninic nappes. The second and third types of satellite basins are represented by thick clastic wedges located rather far from the tip of the Apenninic nappes. In both cases the clastic wedge, bottom-limited by a diachronous basal unconformity, rapidly thins toward the outer flank of the basin by means of intraformational progressive unconformities. The basic difference between these two latter types of satellite basins is represented by the relative position of the active leading edge, which was located behind and in front of the basin respectively. This discrimination, very important for a step-by-step reconstruction of the kinematic evolution of the thrust belt, may be very difficult if the original tectonic setting has been obliterated by subsequent compressional deformation.